APPENDIX A-1

Review of near- and far-field modeling studies by Stantec Consulting for the Northern Pulp effluent treatment facility replacement project

Prepared by:
Oliver Fringer, Ph.D.
San Francisco, CA, USA

March 7, 2019

Table of Contents

1. Executive Summary

This report provides a review of computer modeling of the fate and transport of effluent from proposed discharge locations in and around Pictou Harbour and offshore of Caribou Harbour near Pictou, Nova Scotia. The modeling work was carried out by Stantec Consulting for assessment of the Replacement Effluent Treatment Facility Project registered by Northern Pulp Nova Scotia Corporation. Simulations were conducted with accepted industry-standard models including the near-field CORMIX model and the far-field MIKE 21 model.

Owing to several problems related to the implementation of the CORMIX and MIKE 21 models, they overestimate the near- and far-field mixing and dilution of the effluent from the proposed outfalls, including the final outfall at site CH-B offshore of Caribou Harbour. This leads to the incorrect conclusion that the environmental impacts will be negligible because the effluent concentrations are predicted to be unphysically low. Instead, correct implementation of the models with more conservative and physically realistic scenarios would show that effluent concentrations in the region could be much larger and that effluent accumulation in Pictou and Caribou Harbours is likely.

The principle problems related to the far-field MIKE 21 modeling include:

1) Agreement between the model simulated currents and water levels and observed currents and water levels in Pictou Harbour is poor. Therefore, we can have no confidence that the model accurately predicts the far-field fate and transport of the effluent at any of the proposed outfall locations.

2) Use of the two-dimensional MIKE 21 model is inappropriate given the potentially strong vertical variability of currents driven by winds and river inflows in the region. These three-dimensional effects can significantly impact the far-field transport by exaggerating accumulation in Pictou and Caribou Harbours.

3) The far-field model scenarios using MIKE 21 omit or incorrectly simulate the impacts of winds, river inflows, offshore currents in the Northumberland Strait, ice, waves, and storm surge. These processes may significantly impact far-field mixing and dilution of effluent and lead to higher effluent concentrations throughout the region.

4) The figures showing maps of low effluent concentrations offshore of Caribou Harbour are misleading because the far-field model artificially dilutes the effluent. Nevertheless, the dilution factors are reported to be over 100 in most of the region surrounding the CH-B outfall, which is an overly optimistic result.

The principle problems related to the near-field CORMIX modeling include:

1) The ambient tidal current used to drive the CORMIX model offshore of Caribou Harbour is much stronger than the expected current during a neap tidal period. Tidal currents are even weaker during winter when there is ice cover which decreases the strength of the tides. Overestimation of the tidal currents gives an unrealistic overprediction of the near-field mixing and dilution of effluent, particularly during slack tides.

2) The ambient density employed in the CORMIX model is too saline because it does not take into account potential effects of river inflows. This makes the receiving waters too dense and leads to too much buoyancy-driven mixing of the effluent plume, thus leading to an overestimate of the near-field mixing and dilution. The CORMIX modeling also ignores the effect of vertical variability in salinity, which could be strong during periods of high river inflows and reduce the near-field mixing and dilution because fresh water layers near the surface may trap the effluent beneath them.

It should be noted that these problems are related to the implementation and choice of models, not to the models themselves. When implemented correctly, CORMIX and far-field models like MIKE 21 or its three-dimensional counterpart, MIKE 3, yield very reliable near- and far-field predictions of effluent transport.

2. Introduction

2.1. Overview

In this report I review the near- and far-field modeling studies conducted by Stantec Consulting to understand the fate of effluent from proposed outfalls located in and around Pictou and Caribou Harbours which are connected to the Northumberland Strait in Pictou County, Nova Scotia, Canada. These studies are part of the Environmental Assessment of the Replacement Effluent Treatment Facility Project registered by Northern Pulp Nova Scotia Corporation (Northern Pulp). Specifically, in this report I analyze the modeling studies contained in the following appendices included in the Environmental Assessment:

1) Appendix E1 – Stantec final Caribou discharge receiving water study (The final study)
2) Appendix E2 – Stantec response to questions
3) Appendix E3 – Stantec receiving water study effluent treatment plant replacement (The preliminary study)

In the preliminary study (Appendix E3), scenarios were conducted to study the effluent transport from two outfalls in (sites Alt-A and Alt-B) and offshore of (sites Alt-C and Alt-D) Pictou Harbour. It was deemed that the suggested outfall location Alt-D was not appropriate because of the potential for ice scour of the outfall in the relatively shallow water (11 m). The final study (Appendix E1) was then undertaken to assess the effluent transport from outfalls located offshore of Caribou Harbour in 20 m of water at sites CH-A and CH-B. Site CH-B was recommended as the location with the least environmental impact. In what follows, I will refer to these appendices as the “final study”, the “response to questions”, and the “preliminary study”. Collectively, they will be referred to as “the studies” or “the Stantec studies”.

Simulating the transport and fate of effluent from a coastal wastewater outfall requires two kinds of models. Roughly within 100 m of the outfall, effluent is diluted relatively rapidly by mixing with ambient ocean waters. This mixing is due to strong turbulence related to jet-like flow from the outfall ports and buoyancy arising from the difference in density between relatively warm and fresh effluent and colder and saltier receiving waters. In the studies reviewed here, this dilution process is simulated with CORMIX (Jirka et al. 1996), an industry standard near-field model that takes into account diffuser geometry and properties of the effluent and receiving waters. After the near-field turbulence and buoyant mechanisms have decayed, the fate and transport of the effluent is dictated by the larger-scale circulation in the coastal region surrounding the outfall. The far-field currents, salinity, and temperature are obtained with a hydrodynamic model that computes circulation in response to winds, tides, river inflows, and other relevant coastal processes. These currents are then used to compute the far-field transport and fate of the effluent. In the studies reviewed here, the MIKE 21 model (DHI 2017) was used to compute the far-field circulation and transport. This model is also an industry standard that has been applied extensively to study circulation and transport in coastal regions. While the CORMIX model is an appropriate choice for the near-field modeling, the MIKE 21 model is not appropriate for this study because it is a two-dimensional model, as discussed in Section 3.1 below.

It is common practice to use far-field models to supply ambient currents and environmental parameters like temperature and salinity to the near-field model. The near-field dilution results including the near-field concentration and vertical distribution of the effluent plume can be supplied to the far-field model. In the Stantec studies, the ambient currents needed for the CORMIX model are taken from the MIKE 21 model, while the ambient density field for CORMIX is taken from measurements of temperature and salinity. The far-field MIKE 21 model does not use results from CORMIX. This is common given that only relative concentrations are needed to assess the far-field dilution when using a two-dimensional model like MIKE 21. As will be discussed in this report, however, a three-dimensional far-field model is needed, and this model requires information about the vertical distribution of the effluent plume from the near-field model.

2.2. Currents and dispersion in the coastal ocean

In coastal areas like the regions in and around Pictou and Caribou Harbours, the currents arise from a multitude of processes, although a simple categorization is to distinguish between the tides and all other non-tidal processes, such as wind-driven, river-driven, and large-scale ocean currents in the Northumberland Strait. A prevailing and misleading theme in the Stantec studies is the suggestion that, although some non-tidal processes are included in the modeling (albeit incorrectly), these non-tidal processes are not important because the tidal currents dominate the near- and far-field effluent transport. However, as discussed throughout this review, the non-tidal processes are extremely important for predicting the fate of the effluent in both the near-field and far-field.

Because of their oscillatory motion in time, tides transport effluent back and forth over an outfall, and with each oscillation the effluent is dispersed, leading to horizontal spreading of the effluent plume. This so-called tidal dispersion is strongest in regions where the tidal currents are both large and vary strongly in space, such as at the mouths of Caribou and Pictou Harbours. Although an outfall plume will spread due to tidal dispersion, there will not be much dilution of the effluent after many tidal cycles unless there are non-tidal currents that can transport the effluent away from the outfall. Without non-tidal currents, effluent would simply accumulate around outfall location CH-B and in nearby Caribou Harbour.

Accumulation of effluent in the vicinity of an outfall is strongest during slack tides, periods of low or negligible currents that occur twice during every tidal period, which is approximately 12 hours (the tidal period due to the moon is 12.42 hours and that due to the sun is 12 hours). The effects of slack tides are most pronounced during neap tides when tidal currents are weakest. For example, the maximum neap tidal current is approximately 10 cm/s at outfall location CH-B (based on the discussion presented in Section 4.2 below). With this tide, the tidal currents will be weaker than 2.5 cm/s for the one-hour period surrounding slack, or for approximately two hours (17%) of the entire tidal cycle. During each one-hour slack tide period, 173 kg[1] of suspended solids would be discharged into the ocean from outfall CH-B. The solids that were discharged 30 minutes before slack tide would find themselves just 45 meters from the outfall, only to be transported back over the outfall again at the end of the next 30 minutes to be re-entrained into the outfall plume. This demonstrates the importance of slack tide in the accumulation of effluent over an outfall diffuser due to the prolonged periods of relatively weak currents, particularly during the neap period of the spring-neap tidal cycle. Furthermore, owing to the reduction in vertical turbulent mixing because of the weak currents during slack tides, there is a strong potential for the suspended solids in the effluent to settle out of the water

---

[1] Based on a concentration of 48 mg/L and effluent flow rate of 1 m^3/s, from Table 3.2 of the final study.

column and onto the bed in the vicinity of the outfall. The effects of slack tides and the potential for settling of suspended solids is not discussed in the Stantec studies.

Fortunately for the health of coastal ecosystems, non-tidal currents exist to varying degrees in all coastal regions. In fact, the tides themselves produce non-tidal currents, much like ocean swell waves produce rip currents that have no wave-like signature. Non-tidal currents that are produced by the tides are generally smaller than other non-tidal currents in the region, such as wind-driven, river-driven, and large-scale ocean currents. While river flows and winds are included in the far-field modeling, these effects are not accurately simulated, as discussed in Section 3.1 below. There are large-scale ocean currents that are predominantly from the west to east in the Northumberland Strait at speeds ranging from 6-9 cm/s (Lauzier 1965). Another non-tidal current in the region is the counterclockwise circulation around Pictou Island that has been observed by local fisherman (MacCarthy and Egilsson 2019). This non-tidal current is likely driven by a combination of winds and tides. Although they are important in dictating the far-field transport of effluent, these non-tidal currents are regarded as not important and not included in the Stantec studies.

3. Review of the far-field modeling

3.1. Two- vs. three-dimensional modeling

The MIKE 21 model employed in the far-field simulations is not appropriate because it is two-dimensional and does not represent important three-dimensional processes in the region, such as wind-driven circulation and density effects arising from freshwater flows from rivers. A more appropriate model like MIKE 3 would need to be used to account for these effects.

The MIKE 21 model employed by Stantec is a two-dimensional model in that it computes the depth-averaged currents at each grid cell in the computational domain. Therefore, it assumes that the currents are constant with height above the bed in each grid cell. The three-dimensional equivalent of MIKE 21 is the MIKE 3 model (also by DHI), which computes the variability in currents as a function of height above the bed. The principal advantage of two-dimensional, depth-averaged models is that they are computationally efficient because three-dimensional models require addition of grid cells in the vertical direction. In the case of the Stantec simulations, a three-dimensional model would require at least 20 layers in the vertical which would increase the model runtime by at least a factor of 20.

Despite its computational efficiency, a two-dimensional model is not appropriate to simulate the far-field effluent transport because of the importance of three-dimensional processes in the coastal region around Pictou and Caribou Harbours arising from variations in salinity and temperature, which affects the density stratification. Density stratification due to salinity arises along coastlines where river inflows bring fresh water into the ocean. Because the river water is fresh, it is less dense than the salty ocean, thus inducing vertical variations in the salinity field in which the denser, salty water lies beneath the lighter, fresher water above. Temperature stratification also exists throughout the oceans since the upper layers tend to be heated by the sun, leaving warmer and lighter waters above colder and denser waters. Temperature stratification is weakest in winter months when incoming heat is weakest.

Salinity stratification is more important than temperature stratification in coastal waters where river effects can be important. For example, the top and bottom salinities in the Pictou

Road region in July 1995 were 23.7 and 31.2 ppt (parts per thousand by mass), respectively, while the top and bottom temperatures were 13.5°C and 14°C, respectively (Preliminary study, p. 2.21). This translates to a top-bottom difference in density of 5.8 kg/m^3 due to the salinity and 0.1 kg/m^3 due to temperature, using the UNESCO equation of state calculator (UNESCO 1981). In December 1998, the salinity stratification at the same location was weaker (top-bottom salinity difference of 2 ppt) although the temperature stratification was slightly stronger (top-bottom temperature difference of 2°C). The salinity stratification generally increases with increasing river flow and decreases with tidal flow strength, since tidal currents generate turbulence that tends to mix the salinity and temperature field and weaken the vertical density stratification. Measurements indicate that the surface salinity near the East River in the Pictou Harbour region varied from 20 ppt during low-flow periods to just 5 ppt during high-flow periods (Preliminary study, p. 2.21).

Ocean water is generally stratified in the vertical because density increases with depth, with lighter, less dense waters overlying heavier, denser waters. However, in the coastal ocean there is also horizontal variability in the salinity-induced density. At a river mouth, the water is fresh and there is no vertical salinity stratification, while in the ocean far from the river mouth the salinity is high, yet there is also weak vertical salinity stratification. The most important effect of this horizontal variability in density is to induce a three-dimensional circulation in which fresh, river waters flow seaward over denser ocean waters which flow landward. In addition to the implications for the near-field transport (See Section 4.2 below), the implication for far-field transport is that effluent may be transported into the harbours with the landward-flowing denser currents. This effect is accentuated in deeper waters, implying that it will be stronger in Pictou Harbour (which also has higher freshwater flows), although the shipping channel in Caribou Harbour can act as a conduit to transport effluent-rich ocean waters into the harbour.

A second three-dimensional effect that cannot be captured by a two-dimensional model is related to the winds. When aligned with the main axes of Pictou or Caribou Harbours, winds will drive currents downwind along the shallow edges while the flow in the central, deeper portions will be driven upwind. Since the dominant westerly winds (August-April[2]) in the region are generally aligned with the main axes of the harbours, they have the potential to drive surface effluent seaward and that at depth into the harbours. Wind-driven circulation is typically not as strong as that driven by the rivers or tides, although it can be important during periods with neap tides and low river inflows.

A two-dimensional model also cannot capture the variability of the effluent with depth. The assumption of two-dimensionality in the effluent field is reasonable when the three-dimensional effects in the flow field are relatively weak. In fact it is possible to approximate some three-dimensional processes quite well with a two-dimensional model, such as a process known as shear-flow dispersion. Because of bottom friction, currents are slower near the bed, and if there is wind-driven circulation, the currents may be stronger near the surface. Therefore, tracers[3] that are in regions of the water column with slower-moving currents will be transported more slowly in the horizontal than those in the faster-moving regions of the water column. This process can be thought of as horizontal dispersion of the tracer field because it is spreading horizontally, and can be approximated reasonably well in a two-dimensional model with a shear-

[2] https://weatherspark.com/y/28559/Average-Weather-in-Pictou-Canada-Year-Round

[3] A tracer is a substance that is transported passively with the flow without buoyancy effects.

flow dispersion coefficient. The MIKE 21 model includes many approximations like this to account for three-dimensional effects in the two-dimensional transport module, although these were not employed in the Stantec studies (Preliminary study Table 2-1; Final study Table 2-11: "No decay and no dispersion in the particle tracking module"). Indeed, these approximations are not suitable for estuarine environments given that they work best in riverine environments that are weakly stratified, weakly wind-driven, and lack tidal influence.

Regardless of the influence of dispersion on the two-dimensional transport, the lack of vertical variability in the modeled tracer prevents simulation of an effluent that in reality can vary quite strongly in the vertical. The proposed effluent will typically be less dense than the receiving waters (it is both fresher with a total dissolved solids concentration, or salinity, of 1-4 kg/m^3, and warmer, with a winter temperature of 25^{o}C and summer temperature of 37^{o}C; Preliminary report p. 3.54). Therefore, if the receiving waters are sufficiently salty and cold (See Section 4.2 below) the effluent is expected to rise to the surface and propagate as a surface plume that is just 1-2 m thick based on the CORMIX near-field results in the Stantec studies. Furthermore, the depth at which the plume propagates is not necessarily at the surface, particularly under high flow conditions in which the effluent may be more dense than the receiving waters (See Section 4.2 below). Therefore, it is possible that the effluent could be driven in a direction that is opposite to that in a two-dimensional model if a three-dimensional model were used.

In summary, while three-dimensional effects may not be important during some periods of the year, such as during periods of low river flows and weak winds, in general a three-dimensional model is needed to accurately simulate the far-field fate and transport of effluent from the proposed discharge locations. Indeed, the MIKE 21 manual (Page 2 of DHI 2017) states, "In water bodies with stratification, either by density or by species (ecology), a 3D model should be used. This is also the case for enclosed or semi-enclosed waters where wind-driven circulation occurs." One might argue that three-dimensional models take too much time to run because of the need to include many grid points in the vertical. However, the Stantec final study employed a computational mesh with 24,645 grid cells (15,872 were employed in the preliminary study). Three-dimensional effects would be resolved with reasonable confidence using 20 or more grid cells in the vertical, which would result in 492,900 grid cells in three dimensions. This problem size is well within the reaches of a model like MIKE 3 using modern desktop computers and is relatively low compared to the problem size in other modeling studies in which three-dimensionality is important, both for consulting and academic projects (see, e.g. MacWilliams et al. 2008). Therefore, Stantec should have used a three-dimensional model like MIKE 3 because the circulation in the region is highly three-dimensional and the computational overhead is not restrictive.

3.2. Model setup and forcing

Although rivers and winds are included in the MIKE 21 model, these have no bearing on the far-field results because the effects of winds and rivers are not correctly reproduced with a two-dimensional model. Other processes like waves, storm surges, and large-scale currents were also not included in the MIKE 21 model even though they are important. Finally, the MIKE 21 simulations were conducted over a one-month period which is not long enough to assess the potential for effluent to accumulate in the harbours over much longer periods.

Data from tidal, wind, and river inflow measurements were supplied to the MIKE 21 model using standard practices in coastal ocean modeling. However, owing to the two-dimensional nature of the model, the winds and river inflows have little to no bearing on the far-field results in the studies. Wind and river inflow data could be supplied to a three-dimensional model in a similar manner as it was supplied to the MIKE 21 model in the studies, although estimates for flows in all rivers and streams would need to be included (only the East River was included). As suggested in the Stantec studies, river inflows should be based on stream gauges when available, and based on approximations using the relative catchment area when unavailable (the East River inflow was inferred from measured flows in the Middle River at the Rocklin hydrometric station). With regard to tidal forcing, the standard practice was performed in which the observed tides at Wood Islands were reconstructed based on superposition of the most important components of the tides (using software such as T_TIDE; Pawlowicz 2002). However, the reduction in tidal amplitudes due to large-scale ice cover was not included in the tidal forcing (See Section 3.4 below).

The influence of wind-generated waves and swells were not included in the MIKE 21 model which is a reasonable assumption, although waves should be included during storms, as should the effect of storm surges (See Section 3.4 below). Finally, the west-to-east currents in the Northumberland Strait at speeds ranging from 6-9 cm/s (Lauzier 1965) should be included. These large-scale currents can have an important impact on transport by flushing a region that might otherwise accumulate with effluent without river flows or winds. While this will contribute to flushing of the proposed outfall at location CH-B near Caribou Harbour, it will drive the effluent southward with the potential to be entrained into Pictou and Boat Harbours. This effect is likely to be pronounced with three-dimensional modeling.

To evaluate the far-field dilution characteristics of effluent discharged from the proposed outfall locations, the MIKE 21 model was run over a total simulation time of one month during July 2016 for each outfall. This length of time is not sufficient to evaluate the effects of the effluent plumes given that the flow of effluent is not yet in equilibrium over such a short time period. The appropriate time period is dictated by the flushing time of the estuaries which can take days to months depending on the tides, river flows, winds, and large-scale circulation in Northumberland Strait. It is impossible to determine equilibrium from the spatial distributions of the effluent dilution factors (such as Figure 2.13 in the final study, showing the spatial distribution of the effluent dilution factor from the CH-B discharge location in the vicinity of Caribou Harbour after one month), since the effluent may still be accumulating in one of the harbours at the end of the month. A quantitative measure would need to be computed to demonstrate that the model is in equilibrium. For example, the total effluent mass in each harbour would need to be relatively constant in time, at least when averaged over a tidal cycle. Variations in forcing from processes that act over intervals that are longer than the tides (e.g. the spring-neap cycle, rainfall and associated river flow events, seasonal variations in winds), lead to associated slow variations in the effluent transport, and so these would need to be accounted for when assessing whether the total mass in the harbours is in equilibrium (see, e.g. Rayson et al. 2016).

In summary, the tides are the only component of the forcing in the far-field simulations that have any significant impact on the far-field dilution results. The other components of the forcing, including wind, river inflows, waves, storm surges, and large-scale currents are either not included or have little to no impact. Accurate representation of all of these effects would need a three-dimensional model that is run for much longer than one month to account for possible accumulation in the harbours.

3.3. Model validation

Model validation is an important step in coastal ocean modeling because it demonstrates that the far-field model accurately predicts realistic currents, water levels, and other parameters. Not only is there no quantitative model validation in the studies, but the comparisons of water levels and currents to observations in Pictou Harbour demonstrate that the MIKE 21 model performs poorly. Therefore, the MIKE 21 model cannot be used to assess, with any level of confidence, the far-field behavior of the effluent discharged from the proposed outfall locations.

Validation is the most important step in coastal ocean modeling because it proves that the model is a faithful representation of what is happening in the real world. This gives the user confidence to use the model to analyze results obtained during the validation period, but more importantly during periods when there is no data so that predictions under a wide variety of scenarios can be made. An important component of validation is the availability of appropriate observational datasets. For two-dimensional modeling, these datasets should include time series of observations of sea-surface height and the east and west components of depth-averaged currents. Depending on the instrument, depth-averaged currents can be computed if the instrument measures currents throughout the water column (such as an acoustic Doppler current profiler, or ADCP), since these measurements can be averaged to produce an accurate representation of the depth-averaged currents. However, it is more common to measure currents at a point above the bed. If three-dimensional effects are weak, then the depth-averaged model result can be validated with the point measurement. Strong three-dimensionality makes it difficult to compare a point measurement to the result from a two-dimensional model, which should not be expected to produce the correct currents when three-dimensional effects are important. Three-dimensional models should be validated with velocity data at different heights above the bed in the water column and with time series of salinity and temperature near the bed and free-surface (to assess model ability to reproduce the stratification). Since three-dimensional models compute the vertical distribution of turbulent mixing, then it is desirable to obtain measurements of turbulence to validate the turbulence models. Ideally, models could validate the results of effluent transport, although such observational datasets are rare and so this is not common.

A common step that is often performed in coastal ocean model validation is what is referred to as calibration, in which model parameters that cannot be measured are varied to improve the results. Despite the availability of accurate bathymetry datasets, the bed roughness is rarely measured although it plays an important role in dictating the resistance by the bed on the flow. For example, beds covered with sands or gravels are rougher than beds that are covered with silts or muds, and so the resistance over sands and gravels should be higher. Sometimes, the roughness may be very large if there are bedforms like sand ripples or dunes. Even the drag by vegetation, corals, and kelp is modeled with an effective roughness (Fringer et al. 2019). In some cases, the roughness is approximated with knowledge of the distribution of sediments (this was accounted for in the near-field CORMIX modeling). However, the bottom roughness is more commonly used as a calibration or tuning parameter and varied to give the best match between observations and simulations. In the MIKE 21 model, the roughness is represented specifically by the Manning's roughness parameter, which is used to compute the drag in flows with a free surface with given bed roughness properties.

After performing the appropriate calibration, it is standard practice to compare observations to simulations with quantitative metrics. There are many metrics available in the literature, although the most common are the mean error (also known as the bias), root-mean-square error, the coefficient of determination ("r-squared") and the lag, which is a measure of the time error between the observations and predictions. Another common metric is the skill score, which is a measure of the simulation error normalized by a measure of the spread in the observations. It is generally agreed upon in the coastal modeling community that a skill score greater than 0.65 characterizes excellent agreement between the model and observations (Allen et al. 2007). For simulations with tides, it is common to compare the amplitudes and phases of observed and modeled tidal constituents of both currents and water levels. These are particularly important to show that the model correctly captures the directions and magnitudes of the tidal currents. Examples of comprehensive validation of three-dimensional estuarine modeling studies can be found in MacWilliams et al. (2008) and Wang et al. (2011).

The MIKE 21 validation presented in the preliminary study by Stantec indicates that the model performs poorly because there is weak agreement between the simulations and observations. The validation is performed by running the model over a period in April 1990 when observations of water levels and currents in Pictou Harbour are available. Some statistics are computed, such as minimum, maximum, mean, and standard deviation, yet these statistics are computed separately for the observations and simulations and provide no objective measures for comparison like those found in the literature and discussed above. Despite a lack of quantitative comparisons, the qualitative comparisons represented by the figures in the preliminary study clearly indicate that the agreement between simulations and observations is poor. For example, Figure 1 below shows a comparison between simulated and measured water levels in Pictou Harbour (Figure 2-8 from the preliminary study). While the agreement in timing of the water level is good, most of the high- or low-water levels (indicated by the horizontal blue lines) are visibly incorrect. This lack of agreement could be due to wind and river forcing that was omitted from the model because of a "…lack of the simultaneous records of wind and river discharge during the period of model calibration in April 1990" (Preliminary study, p. 2.27). However, wind or flow events would produce disagreement in the tides over the duration of these events (over a few days each, such as during April 17-21), not throughout the entire record. Furthermore, attributing errors to incorrect forcing implies that the validation period is inappropriate because it does not allow for a demonstration of model fidelity through proper validation. Comparison of observed and simulated currents in Pictou Harbour in Figure 2-9 of the preliminary study shows that the model underpredicts the current speeds by roughly 20% at Location #1 and roughly 50% at Location #2, and in some cases by 80%. This level of disagreement is unjustifiable. Furthermore, there is no indication that the model correctly simulates the direction or timing of the currents since only current speeds are compared.

The differences between observations and simulations is attributed to "the nature of stratified currents through the water column from surface to the seabed, as well as the difference in bathymetry between the existing condition and that in 1990" (Preliminary study, p 2.28). If the difference is indeed due to stratification effects, then this justifies the need for a three-dimensional model. Differences in bathymetry would indicate that the choice of the validation period is not suitable because the circulation in the region was fundamentally different in 1990 than it was when the bathymetry datasets were collected over the past decade. Of course, it is always desirable to use more recent observations to ensure that the results are not contaminated by differences between the dates in which the bathymetry and flow measurements were made. However, a more careful validation procedure and use of an appropriate model should be able to indicate whether this is the case and if more recent data is needed. Regardless, the bottom line is that simply more observations are needed to prove that the model simulations are accurate. Even if the validation indicated that the simulations of currents and water levels in Pictou Harbour were excellent, it would be difficult to argue that the model also correctly reproduced currents in and around Caribou Harbour unless there were observations of water levels and currents from at least one station in that region.

In summary, the validation suggests that the model does not correctly predict the magnitude, direction, or timing of the currents. Therefore, in addition to a lack of validation in or near Caribou Harbour, the results provide no confidence that the model can accurately compute the currents and simulate the subsequent far-field fate and transport of the effluent from any of the proposed outfall locations. Furthermore, the validation provides no measure of confidence that can be ascribed to the predictions of ambient currents or directions at any of the six sites for use in the near-field modeling studies (See Section 4.2 below).

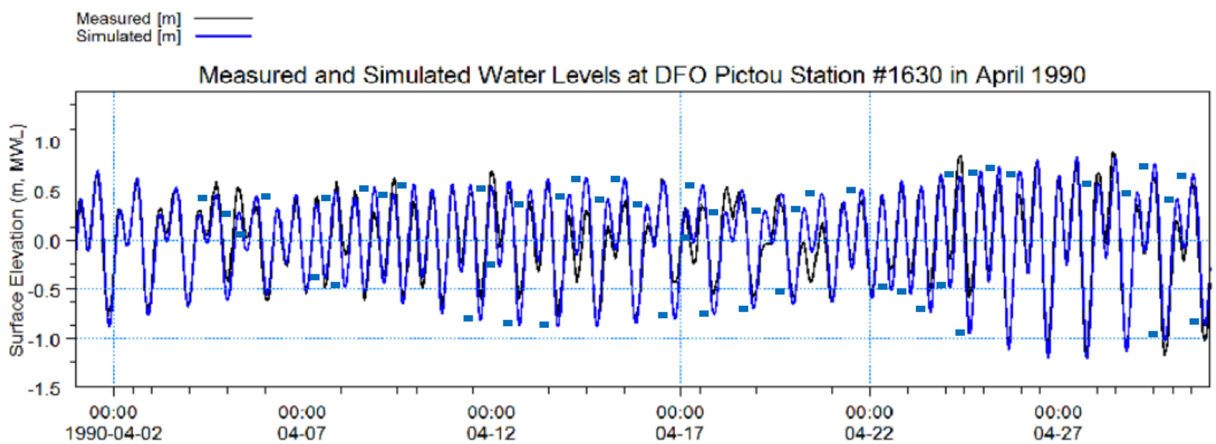

Figure 1: (Figure 2-8 from the preliminary study): Comparison of simulated to measured water levels in Pictou Harbour during April 1990. The blue horizontal lines were added to indicate incorrectly predicted low or high water levels.

3.4. Model scenarios

The scenarios that were conducted in the studies could only evaluate (unsuccessfully) the effect of the tides in a two-dimensional model. Many more scenarios are needed using a three-dimensional model to assess the potential impacts of winds, river inflows, large-scale currents in the Northumberland Strait, waves, storm surges, and ice during winter.

The far-field model scenarios in the studies were carried out with environmental conditions that are stated to minimize mixing of the effluent plume, thus producing conservative results. The conditions include use of “smaller tidal ranges, warmer ambient waters, less wind-driven surface currents, and lower freshwater flows from rivers” (Final report, p. 3). Warmer ambient waters during summer are conservative because, “in winter, mixing is effectively enhanced due to the larger difference in temperature and salinity (density) conditions” (Final report, p. 3). Wave and storm surge conditions are not included in the model given that "surge tides generate turbulence and ultimately provide better and faster mixing conditions" (Answer #2, Response to questions).

While some of these conditions are indeed conservative, not all are relevant or necessarily conservative, particularly in a two-dimensional model. Because the far-field model is two-dimensional and there is no vertical density stratification, the far-field plume dynamics are insensitive to the density of the effluent plume. Therefore, two-dimensional results should be the same for ambient summer or winter temperature conditions. A difference between two-dimensional effluent transport results in summer and winter could, in principle, be based on different initial effluent concentrations derived from the near-field model while taking into account the different ambient conditions from observations. However, the discharged effluent concentration in the far-field model is arbitrary because the dilution factor is a ratio of the far-field to discharged effluent concentration, and thus the actual concentration discharged from the outfall is irrelevant. A reduction in tidal and wind-driven currents reduces the vertical mixing of the plume, although again this has no bearing on the far-field results because the plume is vertically well-mixed in the two-dimensional model. However, different tidal conditions affect the tidal dispersion in the two-dimensional model and thus the tides have a significant impact on the far-field results. Wind-driven currents also affect the far-field results, but these effects are weak in a two-dimensional model since it does not account for wind-driven recirculating currents. Smaller river inflows may also be more conservative because they would be less likely to flush effluent out of the harbours. However, wind and river inflow effects can only be correctly simulated with a three-dimensional model, since both winds and river inflows can transport effluent into the harbours (See Section 3.1 above). Finally, while waves and storm surges indeed provide more mixing and dilution in the near-field, the surge has the potential to transport offshore effluent into the harbours, thus it may potentially be less conservative in terms of far-field transport.

Ice plays a significant role in the circulation and far-field effluent transport in coastal areas like Pictou and Caribou Harbours, yet its effects were not incorporated into the MIKE 21 model in the Stantec studies. While there are frameworks that can couple a model for ice formation and melting to a model like MIKE 21 (e.g. Kusahara and Hasumi 2013), it is possible to approximate the effects of ice sheets by imposing friction at the ice-water interface in the circulation model that impedes the flow of water due to the friction from the ice (Georgas 2012). In smaller domains like those in the Stantec studies, in addition to friction from the ice, the tidal boundary conditions must be altered to account for the significant reduction in tidal amplitude due to ice cover over the Gulf of St. Lawrence (Smith et al. 2006). Alternatively, these boundary conditions must be obtained from data measured during winter when there is large-scale ice cover. In shallow areas, the flow may be completely blocked when ice freezes over the entire water column, in what is referred to as "fast ice" by fishermen in the Pictou area (MacCarthy and Egilsson 2019). In the final Stantec study (p. 3), it is indicated that a winter scenario and the associated effects of ice are not considered because "the presence of ice cover would increase turbulence at the ice/water interface by providing resistance to the ambient water currents, resulting in higher mixing and dilution". Indeed, higher mixing and dilution may take place and can be modeled in the near field with CORMIX, but turbulent mixing at the ice/water interface is not accounted for in the far-field model because it is two-dimensional. Instead, the effect of ice in the far-field model is to reduce the magnitude of the currents and reduce the potential for far-field dilution. Therefore, a winter model run with extensive ice cover and appropriate boundary conditions is needed to represent a worst-case scenario for the far-field dispersion despite the substantial initial dilution of the strongly buoyant effluent during this period.

Overall, the scenarios in the Stantec reports do not reproduce the impact of different physical processes over the course of the year on the effluent transport in the region. In its current form, the far-field model can only be used to simulate the influence of tides on the far-field dispersion of the effluent plumes during low flow and low wind conditions in the absence of ice and large-scale currents. To obtain a good understanding of all of the possible scenarios that might impact the far-field transport, a three-dimensional model would need to be run under scenarios that demonstrated the effects of (1) strong/weak winds, (2) strong/weak river flows, (3) with/without ice cover (including the associated weaker tidal forcing and possibly fast ice), and (4) with/without large-scale currents through the Northumberland Strait. In each of these scenarios, the model would need to be run for at least as long as the flushing time to ensure that the far-field effluent field reaches equilibrium. If the flushing time is not much longer than a spring-neap tidal cycle, then additional scenarios would need to be run to understand the impact of strong (spring) vs. weak (neap) tides. The freshwater inflows would need to include all possible rivers and effluent from municipal wastewater treatment plants, given that the worst-case scenario may include freshening of the receiving waters to a point that significantly impacts the near-field dilution (See Section 4.2 below). Finally, storm surge scenarios would need to be studied given the possibility of strong waves and surges in the region, which could lead to significant accumulation in the harbours.

3.5. Results

The particle tracking module in MIKE 21 over-approximates the far-field mixing and dilution because of the assumption of uniformly distributed effluent mass throughout the volume of each grid cell. This gives the best-case scenario because it mixes the effluent from a point discharge completely over the water column, thus eliminating the possibility of higher concentrations confined to near-surface or mid-water layers of effluent. As a result, the assessment by Stantec that the far-field dilution factors for most of the region surrounding site CH-B are above 100 at the end of the one-month simulation period is overly optimistic. Accounting for vertical variability in the plume could lead to much smaller dilution factors but this would require a three-dimensional model. Dilution factors are also over-approximated in Caribou Harbour because the simulations are not run for long enough time to allow for accumulation of effluent in the harbour due to tidal dispersion.

As they are presented in the reports, the far-field modeling results provide only qualitative, and in some cases misleading, information about the far-field fate and transport of effluent from the proposed outfalls. The focus of this section is on Figures 2.5-2.13 in the final study, which depict extremely low concentrations of the effluent field around site CH-B. For example, in Figure 2.5 there is a small patch of effluent located over the outfall which appears to have a concentration of 2-3 mg/L. It is hard to imagine how the concentration of the effluent from the outfall could have diluted by nearly a factor of 50 (from 100 mg/L) even though this figure depicts the concentration field at slack tide during a neap tidal cycle. As discussed in Section 2.2 above, during slack tide we expect higher concentrations due to buildup of effluent because currents are too weak to induce any significant transport away from the outfall. Higher effluent concentrations are also expected because turbulent dispersion is ignored in the particle tracking module of MIKE 21 to promote conservative dilution factors. It is possible that a diluted concentration from the outfall is imposed in the far-field model based on the near-field modeling results, although an arbitrary concentration of 100 mg/L is assumed given that the relative concentration is of interest.

The low concentrations in the figures can be explained by the particle tracking module that is used to transport effluent in MIKE 21. In the particle tracking module, the outfall is modeled as a point source from which particles with a given amount of mass are released at specified time intervals. After being released, the particles are transported by currents computed with the MIKE 21 hydrodynamic module. In the Stantec final study, the mass flow rate from the outfall is given by 0.1 kg/s, based on the assigned concentration of 100 mg/L and flow rate of 1 m^3/s. Therefore, if we assume that one particle is released from the outfall every hydrodynamic time step of 60 s (the details of how often particles are released are not provided, although this is a safe assumption), then it must be assigned a mass of 6 kg. It is possible to release particles at shorter intervals or multiple particles at each time step, with mass divided equally among the particles to ensure the same prescribed mass flow rate of 0.1 kg/s. However, there would be no difference between transport of a single particle and a group of particles because particles in a group do not spread over time due to a lack of turbulent dispersion, which is ignored by Stantec in the particle tracking simulations. In addition to a lack of dispersion, there is no decay assigned to the particles in the Stantec studies, and hence the mass of each particle remains fixed during the simulations.

To convert the distribution of particles to a concentration field on the hydrodynamic grid, the total mass in each grid cell (which is the sum of the masses of all of the particles in each cell) is divided by the volume of the grid cell. Assuming the grid resolution around site CH-B is approximately 25 m (based on the mesh shown in Figure 2.3 in the final study), then the volume of the prismatic grid cell containing the point release at the location of outfall CH-B is approximately 6000 m^3, based on a depth of 20 m and cross-sectional area of approximately 300 m^2. The minimum concentration in this cell can be estimated by assuming it is empty and then filled with 6 kg of effluent after one 60-s time step. Since it is assumed that this mass is uniformly distributed over the cell volume, the resulting effluent concentration will be 1 mg/L, implying a dilution factor of 100 relative to the assumed inflow concentration of 100 mg/L. This shows that conversion of the particle mass to a concentration field results in artificial mixing of the effluent, giving rise to effective mixing and dilution that depend to great extent on the mesh resolution, depth, and details of the particle release at the outfall (i.e. particle release time interval, mass per particle, number of particles per interval). Although these details are not provided in the Stantec studies, it is clear that much of the far-field dilution is an artifact of the way in which the concentration fields are calculated.

The artificial dilution arising from two-dimensional particle tracking simulations like that in the MIKE 21 model is a common feature of coastal ocean modeling. It is possible to reduce the dilution by increasing the particle release rate or by decreasing the grid size. However, decreasing the grid size is often difficult given computational constraints associated with far-field studies on grids that are finer than those in the Stantec studies. Regardless of grid resolution or the details of the particle tracking module, conclusions about far-field mixing and dilution derived from particle tracking results in a two-dimensional model should take the inherent overestimation of mixing and dilution factors into account. In this regard, Figures 2.5-2.13 in the final study cannot be used to conclude that the environmental impacts of the effluent from outfall CH-B are negligible simply because the dilution factor is at least 100 in most of the domain at the end of the 1-month period. Instead, these dilution factors represent the best-case scenario in which the effluent is mixed over the water column instantaneously upon being released from the outfall. Owing to the buoyant nature of the near-field plume and other three-dimensional effects, the effluent could be confined to a layer much smaller than the depth (as discussed in Section 3.1). As indicated by the near-field modeling results in the final study, this layer can be as small as 1-2 m, which would lead to a reduction in the dilution factor in the region surrounding the CH-B outfall by a factor of 10 or more because the effluent is not completely mixed over the water column. A three-dimensional model would be able to account for the vertical variability of the effluent plume through use of the near-field model to inform the vertical variability in the vicinity of the outfall. This would reduce the artificial dilution associated with the assumption of complete mixing over the water column in a two-dimensional model.

An additional perplexing aspect of Figures 2.5-2.13 in the final study is that they appear to depict transport of patches created by pulses of effluent discharges rather than trails of effluent emanating from the continuous-in-time discharge at outfall CH-B. Examples of such an effluent field showing trails emanating from the outfall locations are depicted in Figures 2-20 and 2-21 from the preliminary study, which show the effluent concentration field surrounding sites Alt-C and Alt-D near Pictou Harbour. Effluent trails are not visible around site CH-B in Figures 2.5-2.13 from the final study because the overestimated dilution due to the particle tracking module produces concentrations in the trails that are too low to be visible with the given color scale. Instead, higher-concentration patches (that also have artificially low concentrations) oscillate with the tides while slowly propagating away from the outfall with the weak non-tidal flow produced by the tides (see Section 2.2 for a discussion of tidal vs. non-tidal flows). While these simulations indicate that there is some dilution of the effluent patches since their concentrations decay in time, the dilution is representative of the best-case scenario when compared to the effluent concentration at the outfall of 100 mg/L.

Another process that is likely reducing dilution factors but is not represented in the simulations is accumulation in Caribou Harbour. Figure 2.11 in the final study clearly shows a patch of effluent in the harbour at slack high tide, indicating that it was transported into the harbour during the previous flood tide. Although the patch appears to be leaving the harbour during the subsequent ebb tide (Figure 2.12 in the final study), tidal dispersion is expected to transport effluent into the harbour over many tidal cycles. Furthermore, although inclusion of turbulent dispersion in the particle tracking module would act to dilute the patches, it would accentuate the tidal dispersion and promote transport into the harbour, thereby reducing the dilution in the harbour after many tidal cycles. As discussed in Section 3.4, accumulation in Caribou Harbour would need to be quantified with simulations that were run for sufficient time to demonstrate that the effluent mass in the harbour was not changing in time.

In summary, when computing concentration fields from the particle tracking results, uniform and instantaneous mixing over the grid cell volumes leads to artificially low concentrations and high dilution factors associated with far-field effluent transport from site CH-B. While it is impossible to eliminate this effect, it can be thought of as the best-case scenario in which the outfall plume is uniformly mixed over the water column. As demonstrated by the near-field modeling results in the Stantec studies, this is clearly not the case. Instead, the plume is typically confined to a smaller region in the water column, which implies a much smaller dilution factor when compared to that arising from assuming a uniform effluent concentration over the depth. The artificially low concentrations and high dilution factors produce far-field effluent concentrations in the region surrounding the CH-B outfall after a month-long simulation that are greater than 100, which is an overly optimistic result. The artificial dilution eliminates most of the visible effluent in the figures except for a few small patches that oscillate with the tides. Some of these are transported into Caribou Harbour, indicating the potential for accumulation in the harbour due to tidal dispersion, an effect that should be assessed with simulations over much longer time periods than the 31-day simulations conducted in the final study.

4. Review of the near-field modeling

4.1. Overview of CORMIX

The CORMIX model was used to compute the three-dimensional effluent concentration field in the near-field mixing zone, which is generally defined as the region within 100 m of the outfall. Near-field mixing involves detailed flow and turbulence processes over length scales that are much smaller than the grid in the far-field model. Therefore, they cannot be simulated with MIKE 21 and must be modeled with a near-field model like CORMIX. According to the CORMIX model, the "near-field" is defined as the region between the outfall and the point at which the buoyant plume interacts with a boundary, which can be the bed, the free surface or some intermediate layer in the water column. In this near-field region, the plume dynamics are initially dictated by the high velocity flow and turbulence emanating from the outfall ports which rapidly mix the effluent with ambient waters. Once the high momentum fluid has decelerated (typically within 5-10 meters of the outfall ports), buoyancy-driven turbulence and mixing take over as the plume rises to the surface or at some point in the water column where the plume density matches the density in the water. This could be the thermocline (a point below the surface that separates the warmer, surface waters from the colder, bottom waters) or the halocline (a point at which fresher river waters are separated from the denser, saltier ocean waters below). After reaching the surface or intermediate layer, subsequent dynamics are referred to as the "far-field" zone in CORMIX. In this zone, the plume is transported by the ambient currents while spreading laterally due to weaker buoyancy effects. Once the density of the plume mixes with that of its surroundings, it propagates as a passive plume (i.e. no longer spreading due to buoyancy) with the ambient currents while spreading laterally and horizontally due to the ambient turbulence. This stage of plume development is modeled in CORMIX in a way that is similar to how it would be modeled under similar ambient conditions in a three-dimensional circulation model like MIKE 3.

The CORMIX model predicts the shape of the near-field plume in three dimensions based on the relatively complex geometry of an outfall diffuser, including the ability to specify different numbers of ports and the specific geometry of how they are attached to the diffuser pipe resting on the bed. Because CORMIX solves for the plume characteristics in a much smaller area and over much shorter time periods when compared to those in the far-field model, the characteristics of the flow needed to drive CORMIX are much simpler than the boundary conditions needed to drive the MIKE 21 model. As a result, parameters in CORMIX are generally not tuned, unlike the far-field modeling which requires tuning of, for example, the bottom roughness to improve agreement between observed and simulated currents (See Section 3.3 above). Furthermore, validation of CORMIX results is generally not required given that, at least under the scenarios that can be simulated with the CORMIX package, we expect the model to produce a good approximation of the near-field dynamics. The downside to this simplicity is that the results depend critically on choosing the effluent and ambient parameters that are representative of realistic worst-case conditions that would give the least amount of near-field dispersion and thus representative of the most conservative design scenario. As discussed in the next section, the receiving water conditions do not represent worst-case scenarios.

4.2. Near-field results at location CH-B

The receiving water current and ambient density field supplied to the CORMIX model to predict the near-field mixing and dilution at site CH-B are not representative of worst-case scenarios because the current is too strong and the ambient density is too high. This gives an over-prediction of the mixing and near-field dilution within the 100-m mixing zone surrounding site CH-B. The near-field effluent concentrations are expected to be higher, particularly during periods of high river inflows and when the tidal currents are weaker, such as during neap tides or when there is winter ice cover.

In the final study, two scenarios for the near-field mixing at site CH-B were conducted. The only difference between the two scenarios is the use of one port in the diffuser in the first scenario and three ports in the second. The dilution factor for the three-port design was roughly twice as large as that for the one-port design 100 m from the outfall (Table 3.4 in the final study). The three-port design at site CH-B had a dilution factor that was roughly 30% larger than the six-port design at site Alt-D (Table 4.1 in the final study shows results from site CH-B obtained in the final study and results from site Alt-D, which are repeated from the preliminary study). Despite the likely increase in the dilution factor at CH-B with six ports, it was concluded that the three-port design had a favorable seabed footprint with a lower potential to interact with the seabed than the six-port design, and hence the six-port design was not evaluated at site CH-B. Given the incorrect estimates of the worst-case currents and receiving water density discussed below, studies need to be conducted with three- and six-port designs to understand their characteristics under worst-case scenarios, particularly in the presence of vertical density stratification of the water column.

The inputs to the CORMIX model that have the most significant impact on the near-field mixing in the final study are the effluent flow rate and density and the ambient tidal currents and density. The effluent flow rate was fixed at the annual average rate of 0.98 m^3/s, while the effluent salinity was assumed to be 4 g/L = 4 kg/m^3, the densest value in the reported range of 1-4 g/L. The effluent temperature was reported to be 25°C in winter and 37°C in summer. The summer effluent temperature was chosen under the assumption that the plume would be least buoyant in summer when the receiving waters were at their warmest. The values chosen for the effluent salinity and temperature are stated to give an upper bound for its density, thus giving a conservative estimate for the dilution because more buoyancy-driven mixing is expected to take place if the effluent is less dense than the receiving waters. Using the UNESCO equation of state (UNESCO 1981), a salinity of 4 kg/m^3 and temperature of 37°C give an effluent density of 996 kg/m^3, the value used in the final study.

A key assumption in the CORMIX model is that the ambient currents are steady. Therefore, approximations are needed when applying CORMIX to tidal flows that are unsteady in that the ambient currents flowing past the outfall vary in magnitude and direction over the tidal cycle. When currents are weak, the effluent accumulates above the outfall and dilution is poor. However, the worst-case scenario occurs roughly one hour before or after slack tide when currents are weak yet sufficient to re-entrain the effluent that was recently transported away from the discharge location in the opposite direction before slack tide. CORMIX requires information about the tidal period and peak currents and the magnitude of the ambient currents one hour before or after slack tide in order to provide an estimate of the worst-case scenario. The CORMIX manual (Page 33 of Jirka et al. 1996) also recommends that additional scenarios be conducted with tidal currents at intervals of one or two hours at different stages of the tidal cycle to ensure that all possible scenarios are analyzed.

Based on the information provided in the preliminary and final studies, the ambient current supplied to the CORMIX model does not represent the worst-case mixing scenario. The preliminary report mentions the use of tidal information in the CORMIX simulations, stating that, (p. 3.54) "The results are presented for a time step corresponding to 1 hour before slack tide conditions." However, in the final report only average (10 cm/s) and maximum (27 cm/s) tidal currents are supplied based on MIKE 21 simulations in July 2016 at site CH-B. There is no mention of the tidal current speed expected within one hour of slack tide, as needed for the worst-case calculation in CORMIX. Furthermore, simulations are not conducted during different phases of the tidal cycle as suggested in the CORMIX manual. These would demonstrate the impact of current speed and direction on the dilution factor. The direction, in particular, could impact the effect of the diffuser and port alignment relative to the oscillatory flow. An important implication of the worst-case slack tide is that suspended solids may settle onto the bed within 100 m of the outfall because of the weak currents, as discussed in Section 2.2 above. This possibility is not mentioned or modeled in the Stantec studies.

Regardless of whether the details of the tide are incorporated into CORMIX, the ambient currents applied to CORMIX in the final study are too large to represent a worst-case scenario. Based on Figure 2-14 in the preliminary report, which shows the Northumberland Strait water levels over the 31-day MIKE 21 simulation period, the weakest neap tide on July 14 has a tidal range of 0.6 m, which is more than three times smaller than the strongest spring tidal range of 2 m on July 5. Therefore, the average and maximum tidal currents used in the CORMIX scenarios are much larger than they would be in the worst-case scenario because they are impacted by the large spring tides. A more conservative, worst-case tide would be given by the weakest neap tide during the period, since the weaker currents would have significantly less near-field dilution than the average tide over the 31-day period. It is important to note that, given the insufficient far-field model validation presented in Section 3.3 above, the simulations of the currents at CH-B may not be representative of the actual currents. This implies that if the currents are underpredicted in Pictou Harbour, they will not necessarily be underpredicted at site CH-B, and therefore it is not valid to justify use of inaccurate far-field model results based on the notion that the errors would lead to a more conservative worst-case scenario.

The ambient density field supplied to the CORMIX model is equally as important as the ambient currents. Estimates of the ambient density of the receiving waters were based on observations because the far-field model is two-dimensional (See Section 3.1 above). However, because observations of temperature and salinity at site CH-B were not available, the ambient density was based on observations in the Pictou Road region in August 2014 and September 2006 (Appendix B, Preliminary study). In principle, this would provide a conservative receiving water density given the likelihood that the receiving water salinity, and hence its density, was lower in this region due to more inflows into Pictou Harbour than Caribou Harbour. However, as discussed below, this is not the case. Using data from Pictou Road region, the receiving water density was calculated as 1020 kg/m^3 based on a temperature of 17.6^{o}C and salinity of 28 ppt, which are averages of the observations. With these salinities and temperatures, the effluent is (1020 kg/m^3 − 996 kg/m^3) = 24 kg/m^3 less dense than the receiving waters. According to Stantec, this provides sufficient buoyant mixing to produce far-field dilution factors computed by CORMIX that are within established water quality guidelines for the 100-m mixing zone. Owing to the strong near-field mixing by the three-port diffuser, the plume interacts with the bed up to 25 m away from the outfall. However, the dilution factor of 71 at 10 m indicates this should not be a source of concern for this value of the ambient density.

Rather than using average salinity and temperature values of observations for the ambient, a more conservative scenario for the near-field modeling would have been to use the freshest and warmest observations in the region, which should be 23 ppt instead of 28 ppt and 19.4^{o}C instead of 17.6^{o}C (Appendix B, Preliminary study). This would give a receiving water density that is 4 kg/m^3 less dense than the value used in the final study, yielding a less buoyant effluent plume and less near-field dilution. While it is unlikely that the water temperature would be much warmer than 20^{o}C in the region, waters warmer than 20^{o}C would contribute much less to potential reductions in ambient density than lower salinity values. This is because the density can vary by as much as 25 kg/m^3 due to the 0-31 ppt salinity range in the region (based on data from Galbraith et al. 2014), while it can only vary by 3 kg/m^3 due to the 0-20^{o}C temperature range. In fact, the salinity value of 28 ppt that was used for the scenario is close to the maximum observed salinity in the region of 31 ppt, thus reflecting close to the best- rather than worst-case salinity for buoyancy-driven near-field dilution at site CH-B. A worst-case salinity is likely much smaller given that salinity observations in the East River range from 20 ppt during low-flow periods to as low as 5 ppt during high-flow periods (Preliminary study, p. 2.21). Lower salinity values are also likely near Caribou Harbour, although perhaps not as low given that flows into Caribou Harbour are weaker than those into Pictou Harbour. Nevertheless, all inflows in the region are expected to lower the salinity of the receiving waters surrounding the proposed outfalls in the studies.

The effect of salinity on the near-field dilution is weakest in winter when inflows are at their lowest. Combined with the colder receiving waters, winter ambient density scenarios are not needed given their potential to drive more buoyancy-driven turbulence and near-field dilution. However, given the weaker tidal currents due to ice cover in winter, scenarios would need to be conducted with worst-case winter density values for the ambient and effluent combined with model-derived worst-case weak winter tides during the period of peak ice cover.

In addition to the potential for low salinities to impact the near-field dilution by reducing the effluent buoyancy at site CH-B, low salinities indicate the existence of vertical stratification in which fresher, river water overlies saltier, denser ocean water. For example, observations in the Pictou Road region indicate a top-bottom salinity difference in July 1995 of 7.5 ppt (Preliminary study, p. 2.21), which is the dominant driver of the top-bottom density difference of 5.8 kg/m^3 (See Section 3.1 above). The stratification can reduce near-field dilution by trapping the effluent in a layer beneath the ocean surface where the density of the effluent matches that of the water column. Additionally, the trapping leads to far-field transport at depth rather than at the surface, thus having the potential to propagate toward the fresh water source. In the case of site CH-B, this would mean transport of the effluent into Caribou Harbour (See Section 3.1 above for a more thorough discussion of three-dimensional far-field effects). The CORMIX model has the ability to simulate near-field dilution in the presence of vertically-stratified waters, and the manual suggests including these effects when the vertical variation in density is greater than 0.1 kg/m^3 (Page 33 of Jirka et al. 1996), significantly smaller than the observed top-bottom density difference of 5.8 kg/m^3 mentioned above. Therefore, worst-case dilution scenarios at CH-B should be devised that take into account the potential for low salinity and stratification arising from high freshwater inflows in the region. These scenarios would need to be devised using results from three-dimensional, far-field modeling.

5. Summary

The MIKE 21 and CORMIX models were used to simulate the distribution of near- and far-field effluent discharged from proposed outfall locations in and near Pictou and Caribou Harbours. Although there are numerous metrics that are commonly used to validate far-field model results like those in the MIKE 21 simulations, these are not calculated in the study. Instead, only qualitative comparisons to observations are made, and these indicate that the far-field model is poorly reproducing the currents and water levels throughout the domain. Therefore, as it is implemented, the far-field model is inaccurate and cannot be trusted to faithfully represent actual circulation and transport dynamics in the region. Given the strong three-dimensional nature of the circulation and transport dynamics due to the winds and fresh water flows in the region, three-dimensional processes are expected to significantly impact the far-field transport. Therefore, the two-dimensional MIKE 21 model is not appropriate for use in this study.

In addition to the inaccurate nature of the far-field model, the scenarios that are presented are not representative of the multitude of processes that can impact the far-field circulation and effluent transport. While there is some qualitative evaluation of the impacts of tidal currents on the far-field fate of the effluent, the two-dimensional nature of the MIKE 21 model makes it impossible to predict the effects of strong winds or strong river inflows, effects that can significantly impact the far-field dynamics. For example, freshwater flows and wind-driven circulation can drive effluent into Caribou Harbour from site CH-B, leading to more accumulation than what might be predicted by the two-dimensional model. Furthermore, although near-field dilution may be accentuated in winter owing to the stronger temperature difference between the effluent and receiving waters, there is no assessment of the potential worst-case winter scenario in which reduced tidal currents due to ice cover may significantly reduce both near- and far-field dispersion. Similarly, while the turbulence and mixing due to storm surges and waves would likely increase near-field dilution, there are no simulations conducted to assess their impact on far-field transport, including the potential for accumulation of effluent in the harbours. Finally, the simulations are not conducted over sufficiently long time periods that are needed to ensure that the simulated far-field dilution factors are in equilibrium, making it impossible to assess the potential for accumulation of effluent in regions of the domain with weaker dispersion and flushing, such as the harbours.

Qualitative representation of the far-field dilution dynamics around site CH-B in the figures indicates fundamental inconsistencies with how the effluent concentrations are being computed and interpreted. The concentrations are unphysically low because the model assumes uniform effluent concentrations within each grid cell. This leads to an over-approximation of the far-field mixing and dilution and overly optimistic conclusions about the far-field dilution factors in the vicinity of the outfall at site CH-B, which are reported to be above 100 in most of the region after a one-month simulation. In reality, the effluent concentrations can vary significantly in the vertical, since effluent plumes can be confined to layers near the surface or mid-water, leading to higher concentrations and smaller, more realistic dilution factors. Due to the artificial dilution, trails of effluent emanating from the outfall are not visible in the figures because their concentrations are too small to appear with the given color scale. Instead, small patches of effluent oscillate with the tides, with some propagating into Caribou Harbour. These indicate the potential for accumulation of effluent in Caribou Harbour by tidal dispersion, an effect that can only be captured with simulations that are run over much longer time periods.

Based on the near-field results obtained with the CORMIX model in the final study, Stantec concluded that the dilution factors near the outfall located at site CH-B are within established water quality guidelines for the 100-m mixing zone. However, the ambient currents and densities supplied to CORMIX are not representative of worst-case near-field dilution scenarios. The currents are based on the average and peak tidal currents at site CH-B over the 31-day simulation period, which are too high because the data include two spring tides. A worst-case tidal current would be better represented by a neap tide during this period, which has smaller currents and is therefore expected to induce less near-field dilution, particularly when accounting for accumulation during slack tide. Weaker tidal currents due to winter ice cover further reduce the potential for near-field dilution, although this scenario is also not investigated. Finally, despite the potential for settling of suspended solids during slack tides within 100 m of the outfall, this is not mentioned in the Stantec studies.

In addition to the overestimated tidal currents, the ambient density supplied to CORMIX is also not representative of a potential worst-case scenario. The salinity used to compute the receiving water density is more representative of the maximum salinity in the region, which gives an effluent that is far too buoyant and thus an overprediction of the near-field buoyancy-driven mixing and dilution. The worst-case salinity, and hence receiving water density, should be much lower given the potential for high river flows to reduce the salinity in the region. Furthermore, high river flows would produce vertical salinity stratification or layering in which fresh water overlies salt water, an effect that can be included in the CORMIX model and further acts to reduce near-field dilution.

6. References

Allen, J., Somefield, P., and F. Gilbert, 2007, Quantifying uncertainty in high-resolution coupled hydrodynamic-ecosystem models, Journal of Marine Systems, 64, 3–14. (This paper is not freely available, although the skill score value of 0.65 is mentioned by Wang et al. 2011, which is freely available).

DHI, 2017, “MIKE 21/3 Hydrodynamic modelling (HD FM) - MIKE Powered by DHI Short description”, DHI, 14 pp., (https://www.mikepoweredbydhi.com/download/product-documentation).

Fringer, O. B., Dawson, C., He, R., Ralston, D. K., and Y. Zhang, 2019, "NSF Workshop on the future of coastal and estuarine modeling", NSF Workshop Final Report, 45 pp., (https://web.stanford.edu/~fringer/reports/nsf-workshop-final-report-2018.pdf).

Galbraith, P. S., Chassé, J., Nicot, P., Caverhill, C., Gilbert, D., Pettigrew, B., Lefaivre, D., Brickman, D., Devine, L., and C. Lafluer, 2014, Physical oceanographic conditions in the Gulf of St. Lawrence in 2014, Canadian Science Advisory Secretariat (CSAS) Research Document 2015/032, 87 pp., (http://waves-vagues.dfo-mpo.gc.ca/Library/359694.pdf).

Georgas, N., 2012: Large seasonal modulation of tides due to ice cover friction in a midlatitude estuary, Journal of Physical Oceanography, 42, 352–369, (Freely available online).

Jirka, G. H., Doneker, R. L., and S. W. Hinton, 1996, User's manual for CORMIX: A hydrodynamic mixing zone model and decision support system for pollutant discharges into surface waters, DeFrees Hydraulics Laboratory, School of Civil and Environmental Engineering Cornell University, (https://www.epa.gov/sites/production/files/2015-10/documents/cormix-users_0.pdf).

Kusahara, K., and H. Hasumi (2013), Modeling Antarctic ice shelf responses to future climate changes and impacts on the ocean, Journal of Geophysical Research - Oceans, 118, 2454–2475, (Freely available online).

Lauzier, L. M., 1965, Drift Bottle Observations in Northumberland Strait, Gulf of St. Lawrence, Journal of the Fisheries Research Board of Canada, 22 (2), 353-368, (Copy attached).

MacCarthy, A., and G. Egilsson, 2019, Caribou Harbour and Caribou Channel – dynamics, tides, ice, marine species and fisheries, Description of regional features by local fisherman.

MacWilliams, M. L., Salcedo, F. G., and E. S. Gross, 2008, San Francisco Bay-Delta UnTRIM Model Calibration Report, California Department of Water Resources Tech. Rep., 309 pp., (http://www.science.calwater.ca.gov/pdf/iep_sag/POD_UnTRIM_Calibration_Report.pdf).

Pawlowicz, R., Beardsley, B., S. Lentz, 2002, "Classical tidal harmonic analysis including error estimates in MATLAB using T_TIDE", Computers and Geosciences, 28, 929-937, (Freely downloadable software: https://www.eoas.ubc.ca/~rich/#T_Tide).

Rayson, M. D., Gross, E. S., Hetland, R. D., and O. B. Fringer, 2016, "Time scales in Galveston Bay: An unsteady estuary", Journal of Geophysical Research - Oceans, 121, 2268-2285, (Freely available online).

Smith, G.C., F.J. Saucier, and D. Straub, 2006, Response of the lower St. Lawrence Estuary to external forcing in winter, Journal of Physical Oceanography, 36, 1485–1501, (Freely available online).

UNESCO, 1981, Tenth report of the joint panel on oceanographic tables and standards, Technical Report, UNESCO Technical Papers in Marine Science, 36, Paris, 24 pp., (https://unesdoc.unesco.org/ark:/48223/pf0000046148).

Wang, B., S. N. Giddings, O. B. Fringer, E. S. Gross, D. A. Fong, and S. G. Monismith, 2011, Modeling and understanding turbulent mixing in a macrotidal salt wedge estuary, Journal of Geophysical Research - Oceans, 116, C02036, (Freely available online).

APPENDIX A-2

Oliver B. Fringer

Curriculum Vitae

Academic History

2003 Ph.D. in Civil and Environmental Engineering
Stanford University, Department of Civil and Environmental Engineering
Dissertation: Numerical simulations of breaking interfacial waves

1996 Master of Science in Aeronautics and Astronautics
Stanford University, Department of Aeronautics and Astronautics

1995 Bachelor of Science in Aerospace Engineering, *cum laude*
Princeton University, Department of Mechanical and Aerospace Engineering

Employment Record

2011-present Associate Professor (with tenure), Dept. of Civil and Environmental Engineering, Stanford University

2003-2011 Assistant Professor, Dept. of Civil and Environmental Engineering, Stanford University

2006 Engineering Consultant, Chevron Energy Technology Company

2002-2003 Acting Assistant Professor, Dept. of Civil and Environmental Engineering, Stanford University

2002-2003 Lecturer, Depts. of Mathematics and Computer Science, University of the Western Cape, Cape Town, South Africa

2001-2002 Postdoctoral Researcher, Environmental Fluid Mechanics Laboratory, Stanford University

1996-2001 Research Assistant, Dept. of Civil and Environmental Engineering, Stanford University.

1994-1995 Summer Research Assistant, Dept. of Mechanical and Aerospace Engineering, Princeton University.

1993 Summer Intern, U. S. Dept of State, Foreign Building Operations, La Paz, Bolivia.

1992 Summer Intern, U. S. Consulate, La Paz, Bolivia.

Professional Activities

Scientific committees and conference sessions organized

Co-organizer for session, “Internal Waves/Tides and Sediment Processes on Continental Margins”, 2018 Ocean Sciences Meeting.

Co-organizer and chair for session, “Multiscale topographic effects on large-scale flow: From wakes and lee waves to small-scale turbulence and mixing”, 2018 Ocean Sciences Meeting.

Conference Chair, 16th International Workshop on Multi-scale (Un)-structured mesh numerical Modelling for coastal, shelf and global ocean dynamics, Stanford, CA, August 29-September 1, 2017.

Scientific Committee, 15th International Workshop on Multi-scale (Un)-structured mesh numerical Modelling for coastal, shelf and global ocean dynamics, Toulouse, France, September 27-29, 2016.

Scientific Committee, 14th International Workshop on Multi-scale (Un)-structured mesh numerical Modelling for coastal, shelf and global ocean dynamics, Portland, OR, September 28-30, 2015.

Co-organizer for Session, “Measuring and modeling internal waves and the turbulence cascade: a tribute to David Tang”, 2014 Ocean Sciences Meeting.

Organizing Committee, 63rd Annual Meeting of the APS Division of Fluid Dynamics, 2014.

International Scientific Committee, 7th International Symposium on Environmental Hydraulics, Singapore, 2014.

Scientific Committee, 11th International Workshop on Multi-scale (Un)-structured mesh numerical Modelling for coastal, shelf and global ocean dynamics, Delft, Netherlands, 28-30 August 2012.

Co-organizer for Session, “Transport and mixing due to nonlinear internal gravity waves”, 2012 Ocean Sciences Meeting.

Co-organizer for Session, "Mini-Symposium on Computational Strategies for the Simulation of Nonlinear Waves and Turbulence in Environmental Flows", 63rd Annual Meeting of the APS Division of Fluid Dynamics, 2010.

Scientific Committee, Geophysical and Astrophysical Waves, Les Houches, Chamonix, Feb 6-11, 2011.

Scientific Committee, 9th International workshop on Multiscale (Un)-structured mesh numerical Modeling for coastal, shelf, and global ocean dynamics, Cambridge, MA, 17-20 August 2010.

Scientific Committee, Third International Symposium on Shallow Flows, June 2012, U. Iowa.

Scientific Committee, Ninth International Workshop on Unstructured Grid Modeling of Coastal and Ocean flows (2009).

Session organizer and chair (jointly with T. Peacock and D. Farmer) for AGU Fall Meeting Session OS15: "Internal Waves" (2008)

Session organizer and chair (jointly with S. Ramp and J. Lynch) for AGU Ocean Sciences Session O86: " Nonlinear Internal Wave Observations, Dynamics, and Acoustic Impacts" (2008)

International Scientific Committee, 15th Congress of Asia and Pacific Division of International Association of Hydraulic Engineering and Research, Chennai (2006)

Session organizer and chair (jointly with J. Nash) for AGU Ocean Sciences Session OS11J: "Dynamics of highly nonlinear internal waves" (2006)

External thesis evaluator

1. Subasha Wickramarachchi, "The hydrodynamics of two-dimensional oscillating flows over ripples: The effects of asymmetries in ripple shape and currents", The University of Waterloo, 2017.
2. Cintia Luz Ramón Casañas, "Hydrodynamics and mixing at river confluences: On the influence of buoyancy and the tides", The University of Granada, 2016.
3. Mario César Acosta Cobos, "Computational improvement of 3D hydrodynamic semi-implicit models for oceans and continental water simulations", The University of Granada, 2016.
4. Olga Kleptsova, "On techniques for modelling coastal and ocean flows with unstructured meshes", Technical University of Delft, 2013.

Reviewer/advisory service

NERRS Science Collaborative Research & Integrated Assessment Reviewer (2016)

San Francisco Estuary Institute Bay Modeling Advisory Team (2013)

Link Foundation Selection Committee (2013, 2014)

National Science Foundation (NSF) Reviewer, Physical Oceanography Program (2003-)

National Science Foundation (NSF) Panelist, Collaboration in Mathematical Geosciences, Jun 2-4, 2010.

Dept. of Energy (DOE) Computational Science Graduate Fellowship (CSGF) application screening committee, (2009-)

Journal referee

Advances in Water Resources (2009, 2010)
Boundary-Layer Meteorology (2009)
Coastal Engineering (2009)
Communications in Nonlinear Science and Numerical Simulation (2011)
Computers and Fluids (2010, 2011)
Computers and Geosciences (2009)
Continental Shelf Research (2004, 2013)
Deep-Sea Research (2011)
Dynamics of Atmospheres and Oceans (2007)
Ecological Applications (2006)
Environmental Fluid Mechanics (2013, 2015, 2017)
Environmental Practice (2015)
Estuaries and Coasts (2007, 2015, 2016)
European Journal of Mechanics - B/Fluids (2008, 2011)
Flow, Turbulence and Combustion (2013)
Geophysical Research Letters (2008, 2009, 2011, 2012, 2016)
International Journal for Numerical Methods in Fluids (2007, 2008, 2012, 2013, 2015)
International Journal of Computational Methods (2014)
Journal of Computational Physics (2006, 2010)
Journal of Fluid Mechanics (2003, 2006, 2007, 2008, 2010, 2011, 2012, 2013, 2014, 2015, 2016)
Journal of Geophysical Research: Earth Surface (2015)
Journal of Geophysical Research: Oceans (2006, 2007, 2008, 2009, 2010, 2011, 2012, 2013, 2014, 2016, 2017)
Journal of Hydraulic Engineering (2006, 2007, 2009, 2011, 2013, 2014, 2015)
Journal of Hydraulic Research (2013, 2016)
Journal of Hydrodynamics (2012)
Journal of Hydrology (2014)
Journal of Physical Oceanography (2006, 2010, 2011, 2013, 2014, 2015, 2016)
Limnology and Oceanography Letters (2017)
Limnology and Oceanography Methods (2008)
Marine Geology (2012)
Monthly Weather Review (2007)

Nonlinear Processes in Geophysics (2017)
Ocean Dynamics (2010)
Ocean Modelling (2007, 2008, 2010, 2011, 2012, 2013, 2016, 2017)
Oceanography (2017)
Physics of Fluids (2006, 2007, 2008, 2009, 2010, 2011, 2014, 2015)
San Francisco Estuary and Watershed Science (2014, 2016)
The Sea (2017)
Water Resources Research (2013)

Editorial boards

Ocean Modelling – Editor (2018-)

Journal of Water Waves – Associate Editor (2017-)

Environmental Fluid Mechanics (2017-)

University and Departmental Service

Stanford Interdisciplinary Graduate Fellowship selection committee (2017)

Environmental Fluid Mechanics and Hydrology Program Coordinator (2014-)

Chair, Promotion Committee (associate professor) (2014-2015)

CEE Vision Committee (2014-2016)

SOE Undergraduate Council (2013)

Woods Institute EVP Selection Committee (2013-2016)

CEE Undergraduate Curriculum Committee (2012-2015)

CEE ABET Representative for Environmental Engineering Degree (2011-2012)

CEE Faculty search committee (2012)

Premajor advisor (2012-2014)

Faculty Member, Institute for Computational and Mathematical Engineering (ICME) (2003-)

DOE Computational Science Graduate Fellowship (CSGF) coordinator for Stanford University (2004-)

Admissions chair, Environmental Fluid Mechanics and Hydrology Program, Dept. of Civil and Environmental Engineering (2009-2011, 2013, 2016, 2017)

Sophomore academic advisor (2005-2006)

Mechanical Engineering Flow Physics and Computation faculty search committee member (2005)

Freshman academic advisor (2004-2005)

Institute for Computational and Mathematical Engineering (ICME) curriculum committee member (2003-2004)

Center for African Studies (CAS) search committee member for South Africa Teaching Fellowship (2003)

Dissertation Reading Committee Member:

M. Barkdull, (Principal advisor: S. Monismith) Ph.D. 2016.
K. Cheng, (Principal advisor: L. Hildemann) Ph.D. 2010.
M. Chui, (Principal advisor: D. Freyberg) Ph.D. 2009.
K. Davis (Principal advisor: S. Monismith) Ph.D. 2008.
J. Dunckley (Principal advisor: J. Koseff) Ph.D. 2012.
S. Giddings, (Principal advisor: S. Monismith) Ph.D. 2010.
K. Gleichauf (Principal advisor: S. Monismith) Ph.D. 2015
R. Holmes (Principal advisor: L. Thomas) Ph.D. 2016.
J. Krall (Principal advisor: D. Freyberg) Ph.D. 2014
R. Moniz (Principal advisor: S. Monismith) Ph.D. 2014
N. Nidzieko (Principal advisor: S. Monismith) Ph.D. 2009.
T. Reddy, (Principal advisor: K. Arrigo) Ph.D. 2009.
J. Rogers, (Principal advisor: S. Monismith) Ph.D. 2015
L. Samuel, (Principal advisor: S. Monismith) Ph.D. 2014
M. Squibb, (Principal advisor: S. Monismith) Ph.D. 2014
E. Sta. Maria, (Principal advisor: M. Jacobson) Ph.D. 2013
J. Steinbuck (Principal advisor: S. Monismith) Ph.D. 2009.
L. Walter (Principal advisor: S. Monismith) Ph.D. 2011
R. Walter (Principle advisor: S. Monismith) Ph.D. 2014
J. Weitzman (Principal advisor: J. Koseff) Ph.D. 2013
D. Whitt (Principal advisor: L. Thomas) Ph.D. 2014
V. Sridharan (Principal advisor: S. Monismith) Ph.D. 2015
G. Zhao, (Principal advisor: R. Street) Ph.D. 2009.
R. Zeller, (Principal advisor: J. Koseff) Ph.D. 2014.
D. Zheng, (Principal advisor: L. Hildemann) Ph.D. 2016.

University Oral Examination (Chair)

J. Bae, Computational and Mathematical Engineering (2018)
S. Bose, Aeronautics and Astronautics (2012)
P. Constantine, Computational and Mathematical Engineering (2009)
S. Davis, Geological and Environmental Sciences (2008)
H. Hamilton, Aeronautics and Astronautics (2004)
C. Hamman, Mechanical Engineering (2015)
K. Hosseini, Aeronautics and Astronautics (2005)
S. Infeld, Aeronautics and Astronautics (2005)
M. Ji, Mechanical Engineering (2006)
S. Kang, Mechanical Engineering (2008)
S. Kumar, Aeronautics and Astronautics (2012)
M. Lande, Mechanical Engineering (2011)
G. Lotto, Geophysics (2018)
D. Macklin, Bioengineering (2017)
M. McDowell, Materials Science and Engineering (2013)
K. Moffett, Environmental Earth System Science (2010)
M. Mortazavi, Mechanical Engineering (2015)
L. Katrina ole-MoiYoi, E-IPER (2016)
B. Olson, Aeronautics and Astronautics (2013)
D. Phillips, Mechanical Engineering (2012)
B. Saenz, Environmental Earth System Science (2011)
N. Santhanam, Aeronautics and Astronautics (2004)
J. Seo, Mechanical Engineering (2016)
M. Shoeybi, Mechanical Engineering (2010)
V. Somandepalli, Mechanical Engineering (2006)
D. You, Mechanical Engineering (2003)
C. Yu, Aeronautics and Astronautics (2014)

University Oral Examination (Examiner)

L. Samuel, Civil and Environmental Engineering (2014)
I. Benekos, Civil and Environmental Engineering (2005)
N. Grumet, Geological and Environmental Sciences (2004)
P. Ray, Mechanical Engineering (2006)
A. Santoro, Civil and Environmental Engineering (2008)
R. Simons, Civil and Environmental Engineering (2004)
J. Thompson, Civil and Environmental Engineering (2015)

Awards and Honors

Outstanding Reviewer, Ocean Modelling, 2016

Lorenz G. Straub Award for best dissertation by former Ph.D. student Bing Wang, 2011.

Lorenz G. Straub Award for best dissertation by former Ph.D. student Subhas Karan Venayagamoorthy, 2009.

Presidential Early Career Award for Scientists and Engineers (PECASE), Office of Science and Technology Policy, 2009.

Young Investigator Award, Office of Naval Research, 2008.

Frederick A. Howes Scholar in Computational Science, Department of Energy, 2003.

South Africa Teaching Fellow, Department of African and African-American Studies, Stanford University, 2002-2003.

Bibliographical Information

Publications

Author order is based on percentage of work performed or contributed, except for the PI on the project or paper who is typically listed as last author. Ph.D. student names are in bold, supervised postdoctoral researcher names are in italics.

Refereed Journal Publications

1. **K. S. Nelson** and O. B. Fringer, 2018, "Sediment dynamics in wind-wave dominated shallow water environments", J. Geophys. Res.-Oceans, 123, 6996-7015, doi:10.1029/2018JC013894.
2. M. Traer, A. Fildani, O. Fringer, T. McHargue, and G. Hilley, 2018, "Turbidity current dynamics: Part 1. Model formulation and identification of flow equilibrium conditions resulting from flow stripping and overspill", J. Geophysical Research - Earth Surface, 123, 501–519, doi:10.1002/2017JF004200
3. M. Traer, A. Fildani, O. Fringer, T. McHargue, and G. Hilley, 2018, "Turbidity current dynamics: Part 2. Simulating flow evolution toward equilbrium in idealized channels", Journal of Geophysical Research – Earth Surface, 123, 520–534, doi: 10.1002/2017JF004202
4. B. Wang, L. Cao, F. Micheli, R. L. Naylor, and O. B. Fringer, 2018, "The effects of intensive aquaculture on nutrient residence time and transport in a coastal embayment", Environmental Fluid Mechanics, 18 (6), 1321–1349 doi:10.1007/s10652-018-9595-7
5. **K. R. Scheu**, D. A. Fong, S. G. Monismith, and O. B. Fringer, 2018, "Modeling sedimentation dynamics of sediment-laden river intrusions in a rotationally-influenced, stratified lake", Water Resources Research, 54, 4084–4107, doi:10.1029/2017WR021533

6. Y.-J. Chou, K. S. Nelson, R. C. Holleman, O. B. Fringer, M. T. Stacey, J. R. Lacy, S. G. Monismith, and J. R. Koseff, 2018, "Three-dimensional modeling of fine sediment transport by waves and currents in a shallow estuary", J. Geophys. Res.-Oceans., 123, doi:10.1029/2017JC013064
7. M. D. Rayson, G. N. Ivey, N. L. Jones, and O. B. Fringer, 2018, "Resolving high-frequency internal waves generated at an isolated coral atoll using an unstructured grid ocean model", Ocean Model., 122, 67-84, doi:10.1016/j.ocemod.2017.12.007
8. M. D. Rayson, E. S. Gross, R. D. Hetland, and O. B. Fringer, 2017, "Using an isohaline flux analysis to predict the salt content in an unsteady estuary", J. Phys. Oceanogr., 47, 2811-2828, doi:10.1175/JPO-D-16-0134.1
9. **E. T. Mayer** and O. B. Fringer, 2017, "An unambiguous definition of the Froude number for lee waves in the deep ocean", Journal of Fluid Mechanics, 831, doi:10.1017/jfm.2017.701
10. E. Masunaga, O. B. Fringer, Y. Kitade, H. Yamazaki, and S. Gallager, 2017, "Dynamics and energetics of trapped diurnal internal Kelvin waves around a mid-latitude island", Journal of Physical Oceanography, 47, 2479-2498, doi:10.1175/JPO-D-16-0167.1
11. **R. S. Arthur**, S. K. Venayagamoorthy, J. R. Koseff, and O. B. Fringer, 2017, "How we compute N matters to estimates of mixing in stratified flows", Journal of Fluid Mechanics, 831, doi:10.1017/jfm.2017.679
12. **K. S. Nelson** and O. B. Fringer, 2017, "Reducing spin-up time for simulations of turbulent channel flow", Physics of Fluids, 29, 105101, doi:10.1063/1.4993489
13. L. M. M. Herdman, J. L. Hench, O. Fringer, and S. G. Monismith, 2017, "Behavior of a wave-driven buoyant surface jet on a coral reef", Journal of Geophysical Research-Oceans, 122 (5), 4088-4109, doi:10.1002/2016JC011729
14. M. M. Flint, O. Fringer, S. L. Billington, D. Freyberg, and N. S. Diffenbaugh, 2017, "Historical analysis of hydraulic bridge collapses in the continental United States", Journal of Infrastructure Systems, 23 (3), 04017005, doi:10.1061/(ASCE)IS.1943-555X.0000354
15. E. Masunaga, **R. S. Arthur**, O. B. Fringer, and H. Yamazaki, 2017, "Sediment resuspension and the generation of intermediate nepheloid layers by shoaling internal bores", Journal of Marine Systems, 170, 31-41, doi:10.1016/j.jmarsys.2017.01.017
16. **R. S. Arthur**, J. R. Koseff, and O. B. Fringer, 2017, "Local vs. volume-integrated turbulence and mixing in breaking internal waves on slopes", Journal of Fluid Mechanics, 815, 169-198, doi:10.1017/jfm.2017.36
17. J. S. Rogers, S. G. Monismith, O. B. Fringer, D. A. Koweek, and R. B. Dunbar, 2017 ,"A coupled wave-hydrodynamic model of an atoll with high friction: Mechanisms for flow, connectivity, and ecological implications", Ocean Modelling, 110, 66–82, doi:10.1016/j.ocemod.2016.12.012
18. *M. D. Rayson*, E. S. Gross, R. D. Hetland, and O. B. Fringer, 2016, "Time scales in Galveston Bay: An unsteady estuary", Journal of Geophysical Research-Oceans, 121, 2268-2285, doi: 10.1002/2015JC011181
19. E. Masunaga, O. B. Fringer, H. Yamazaki, and K. Amakasu, 2016, "Strong turbulent mixing induced by internal bores interacting with internal tide-driven vertically sheared flow", Geophysical Research Letters, 43, 2094-2101, doi:10.1002/2016GL067812

20. **R. S. Arthur** and O. B. Fringer, 2016, "Transport by breaking internal gravity waves on slopes", Journal of Fluid Mechanics, 789, 93-126, doi:10.1017/jfm.2015.723
21. **P. J. Wolfram**, O. B. Fringer, N. Monsen, K. Gleichauf, D. Fong, and S. G. Monismith, 2016, "Modeling intrajunction dispersion at a well-mixed tidal river junction", 2016, Journal of Hydraulic Engineering, 142(8), 04016019, doi:10.1061/(ASCE)HY.1943-7900.0001108
22. E. Masunaga, H. Homma, H. Yamazaki, O. B. Fringer, T. Nagai, Y. Kitade, and A. Okayasu, 2015, "Mixing and sediment resuspension associated with internal bores in a shallow bay", Continental Shelf Research, 110, 85-99, doi:10.1016/j.csr.2015.09.022
23. *Chou, Y.-J.,* Holleman, R. C., Fringer, O. B., Stacey, M. T., Monismith, S. G., and Koseff, J. R., 2015, “Three-dimensional wave-coupled hydrodynamics modeling in South San Francisco Bay”, Computers and Geosciences, 85, 10-21, doi:10.1016/j.cageo.2015.08.010
24. A. Cortes, M. G. Wells, O. B. Fringer, **R. S. Arthur**, and F. J. Rueda, 2015, “Numerical investigation of split flows by gravity currents into two-layered stratified water bodies”, Journal of Geophysical Research-Oceans, 120, 5254-5271, doi:10.1002/2015JC010722
25. M. H. Alford, T. Peacock, J. A. MacKinnon, J. D. Nash, M. C. Buijsman, L. R. Centuroni, S.-Y. Chao, M.-H. Chang, D. M. Farmer, O. B. Fringer, K.-H. Fu, P. C. Gallacher, H. C. Graber, K. R. Helfrich, S. M. Jachec, C. R. Jackson, J. M. Klymak, D. S. Ko, S. Jan, T. M. Shaun Johnston, S. Legg, I-H. Lee, R.-C. Lien, M. J. Mercier, J. N. Moum, R. Musgrave, J.-H. Park, A. I. Pickering, R. Pinkel, L. Rainville, S. R. Ramp, D. L. Rudnick, S. Sarkar, A. Scotti, H. L. Simmons, L. C. St Laurent, S. K. Venayagamoorthy, Y.-H. Wang, J. Wang, Y. J. Yang, T. Paluszkiewicz and T.-Y. (David) Tang, 2015, "The formation and fate of internal waves in the South China Sea", Nature, 521, 65-69, doi:10.1038/nature14399
26. **K. R. Scheu**, D. A. Fong, S. G. Monismith, and O. B. Fringer, 2015, "Sediment transport dynamics near a river inflow in a large alpine lake", Limnology and Oceanography, 60 (4), 1195-1211, doi:10.1002/lno.10089
27. *M. Rayson*, E. S. Gross, and O. B. Fringer, 2015, "Modeling the tidal and sub-tidal hydrodynamics in a shallow, micro-tidal estuary", Ocean Modelling, 89, 29-44, doi:10.1016/j.ocemod.2015.02.002
28. **R. S. Arthur** and O. B. Fringer, 2014, "The dynamics of breaking internal solitary waves on slopes", Journal of Fluid Mechanics, 761, 360-398, doi:10.1017/jfm.2014.641
29. **S. Vitousek** and O. B. Fringer, 2014, "A nonhydrostatic, isopycnal-coordinate ocean model for internal waves", Ocean Modelling, 83, 118-144, doi:10.1016/j.ocemod.2014.08.008
30. K. Gleichauf, **P. Wolfram**, N. Monsen, O. Fringer, and S. Monismith, 2014, "Dispersion Mechanisms of a Tidal River Junction in the Sacramento-San Joaquin Delta, California", San Francisco Estuary and Watershed Science, 12 (4), doi:10.15447/sfews.2014v12iss4art1
31. R. B. Zeller, J. S. Weitzman, M. E. Abbett, F. J. Zarama, O. B. Fringer, and J. R. Koseff, 2014, “Improved parameterization of seagrass blade dynamics and wave attenuation based on numerical and laboratory experiments”, Limnology and Oceanography, 59(1), 251-266, doi:10.4319/lo.2014.59.1.0251
32. S. Sankaranarayanan and O. B. Fringer, 2013, "Dynamics of barotropic low-frequency fluctuations in San Francisco Bay during upwelling", Continental Shelf Research, 65, 81-96, doi:10.1016/j.csr.2013.06.006

33. **P. J. Wolfram** and O. B. Fringer, 2013, "Mitigating horizontal divergence 'checker-board' oscillations on unstructured triangular C-grids for nonlinear hydrostatic and nonhydrostatic flows", Ocean Modelling, 69, 64-78, doi:10.1016/j.ocemod.2013.05.007
34. R. Holleman, O. B. Fringer, and M. T. Stacey, 2013, "Numerical diffusion for flow-aligned unstructured grids with applications to estuarine modeling", International Journal for Numerical Methods in Fluids, 72, 1117-1145, doi:10.1002/fld.3774
35. **S. Vitousek** and O. B. Fringer, 2013, "Stability and consistency of nonhydrostatic free-surface models using the semi-implicit theta-method", International Journal for Numerical Methods in Fluids, 72, 550-582, doi:10.1002/fld.3755
36. **S. Koltakov** and O. B. Fringer, 2013, "Moving grid method for numerical simulation of stratified flows", International Journal for Numerical Methods in Fluids, 71 (12), 1524-1545, doi:10.2002/fld.3724
37. **S. K. Venayagamoorthy** and O. B. Fringer, 2012, "Examining breaking internal waves on a shelf slope using numerical simulations", Oceanography, 25(2), 132–139, doi:10.5670/oceanog.2012.48
38. G. S. Carter, O. B. Fringer, and E. D. Zaron, 2012, "Regional models of internal tides", Oceanography, 25(2):56–65, doi:10.5670/oceanog.2012.42
39. R. K. Walter, C. B. Woodson, **R. S. Arthur**, O. B. Fringer, and S. G. Monismith, 2012, "Nearshore internal bores and turbulent mixing in southern Monterey Bay", Journal of Geophysical Research-Oceans, 117, C07017, doi:10.1029/2012JC008115
40. S. N. Giddings, D.A. Fong, S.G. Monismith, C.C. Chickadel, K.A. Edwards, W.J. Plant, **B. Wang**, O.B. Fringer, A.R. Horner-Devine, and A.T. Jessup, 2012, "Frontogenesis and frontal progression of a trapping-generated estuarine convergence front and its influence on mixing and stratification", Estuaries and Coasts, 35 (2), 665-681, doi:10.1007/s12237-011-9453-z
41. **D. Kang** and O. B. Fringer, 2012, "Energetics of barotropic and baroclinic tides in the Monterey Bay area", Journal of Physical Oceanography, 42 (2), 272-290, doi:10.1175/JPO-D-11-039.1
42. R.-Q. Wang, A. W.-K. Law, E. E. Adams, and O. B. Fringer, 2011, "Large-eddy simulation of starting buoyant jets", Environmental Fluid Mechanics, 11 (6), 591-609, doi:10.1007/s10652-010-9201-0
43. Simmons, H., M.-H. Chang, Y.-T. Chang, S.-Y. Chao, O. Fringer, C.R. Jackson, and D.S. Ko. 2011, "Modeling and prediction of internal waves in the South China Sea", Oceanography, 24(4), 88-99, doi:10.5670/oceanog.2011.97
44. **S. Vitousek** and O. B. Fringer, 2011, "Physical vs. numerical dispersion in nonhydrostatic ocean modeling", Ocean Modelling, 40 (1), 72-86, doi:10.1016/j.ocemod.2011.07.002
45. **B. Wang**, G. Zhao, and O. B. Fringer, 2011, "Reconstruction of vector fields for semi-Lagrangian advection on unstructured, staggered grids", Ocean Modelling, 40 (1), 52-71, doi:10.1016/j.ocemod.2011.06.003

46. **V. Chua** and O. B. Fringer, 2011, "Sensitivity analysis of three-dimensional salinity simulations in North San Francisco Bay using the unstructured-grid SUNTANS model", Ocean Modelling, 39 (3-4), 332-350, doi:10.1016/j.ocemod.2011.05.007
47. *S. K. Venayagamoorthy*, O. B. Fringer, A. Chiu, R. L. Naylor, and J. R. Koseff, 2011, "Numerical modeling of aquaculture dissolved waste transport in a coastal embayment", Environmental Fluid Mechanics, 11 (4), 329-352, doi:10.1007/s10652-011-9209-0
48. **Z. Zhang**, O. B. Fringer, and S. R. Ramp, 2011, "Three-dimensional, nonhydrostatic numerical simulation of nonlinear internal wave generation and propagation in the South China Sea", Journal of Geophysical Research-Oceans, 116, C05022, doi:10.1029/2010JC006424
49. **B. Wang**, S. N. Giddings, O. B. Fringer, E. S. Gross, D. A. Fong, and S. G. Monismith, 2010, "Modeling and understanding turbulent mixing in a macrotidal salt wedge estuary", Journal of Geophysical Research-Oceans, 116, C02036, doi:10.1029/2010JC006135
50. K. C. Cheng, V. Acevedo-Bolton, R. T. Jiang, N. E. Klepeis, W. R. Ott, O. B. Fringer, and L. M. Hildemann, 2011. "Modeling exposure close to air pollution sources in naturally ventilated residences: Association of turbulent diffusion coefficient with air change rate", Environmental Science and Technology, 45, 4016-4022, doi:10.1021/es103080p
51. **D. Kang** and O. B. Fringer, 2010, "On the calculation of available potential energy in internal wave fields", Journal of Physical Oceanography, 40 (11), 2539-2545, doi: 10.1175/2010JPO4497.1
52. **Y.J. Chou** and O. B. Fringer, 2010, "A model for the simulation of coupled flow-bedform evolution in turbulent flows", Journal of Geophysical Research-Oceans, 115, C10041, doi:10.1029/2010JC006103
53. *M.F. Barad* and O. B. Fringer, 2010, "Simulations of shear instabilities in interfacial gravity waves", Journal of Fluid Mechanics, 644, 61-95, doi:10.1017/S0022112009992035
54. Q. Bechet, A. Shilton, O. B. Fringer, and B. Guieysse, 2010, "Mechanistic modelling of broth temperature in outdoor photobioreactors", Environmental Science and Technology, 44 (6), 2197-2203. doi: 10.1021/es903214u
55. **Y.J. Chou** and O. B. Fringer, 2010, "Consistent discretization for simulation of flows with moving generalized curvilinear coordinates", International Journal for Numerical Methods in Fluids, 62 (10), 802-826. doi:10.1002/fld.2046
56. W. J. Plant, R. Branch, G. Chatham, C. C. Chickadel, K. Hayes, B. Hayworth, A. Horner-Devine, A. Jessup, D. A. Fong, O. B. Fringer, S. N. Giddings, S. Monismith, and **B. Wang**, 2009, "Remotely sensed river surface features compared with modeling and in situ measurements", Journal of Geophysical Research-Oceans, 114, C11002, doi:10.1029/2009JC005440
57. P. Van Gastel, G. N. Ivey, M. Meuleners, J. P. Antenucci, and O. B. Fringer, 2009, "The variability of the large-amplitude internal wave field on the Australian North West Shelf", Continental Shelf Research, 29 (11-12), 1373-1383, doi:10.1016/j.csr.2009.02.006

58. **B. Wang**, O. B. Fringer, S. N. Giddings, and D. A. Fong, 2009, "High-resolution simulations of a macrotidal estuary using SUNTANS", Ocean Modelling, 28 (1-3), 167-192, doi:10.1016/j.ocemod.2008.08.006
59. R.-Q. Wang, A. Law, E. E. Adams, and O. B. Fringer, 2009, "Buoyant formation number of a starting buoyant jet", 2009, Physics of Fluids, 21, 125104, doi:10.1063/1.3275849
60. **Y. J. Chou** and O. B. Fringer, 2008, "Modeling dilute sediment suspension using large-eddy simulation with a dynamic mixed model", Physics of Fluids, 20, 115103, doi: 10.1063/1.3005863
61. **S. M. Jachec**, O. B. Fringer, R. L. Street, and M. Gerritsen, 2007, "Effects of Grid Resolution on the Simulation of Internal Tides", International Journal of Offshore and Polar Engineering, 17 (2), 105-111.
62. **S. K. Venayagamoorthy** and O. B. Fringer, 2007, "On the formation and propagation of nonlinear internal boluses across a shelf break", Journal of Fluid Mechanics, 577, 137-159. doi:10.1017/S0022112007004624
63. **S. K. Venayagamoorthy** and O. B. Fringer, 2007, "Internal wave energetics on a shelf break", International Journal of Offshore and Polar Engineering, 17 (1), 22-29.
64. **S. K. Venayagamoorthy** and O. B. Fringer, 2006, "Numerical simulations of the interaction of internal waves with a shelf break", Physics of Fluids, 18 (1), 077603, doi:10.1063/1.2221863
65. **S. M. Jachec**, O. B. Fringer, M. G. Gerritsen, and R. L. Street, 2006, "Numerical simulation of internal tides and the resulting energetics within Monterey Bay and the surrounding area", Geophysical Research Letters, 33, L12605, doi:10.1029/2006GL026314
66. O. B. Fringer, M. Gerritsen, and R. L. Street, 2006. "An unstructured-grid, finite-volume, nonhydrostatic, parallel coastal-ocean simulator", Ocean Modelling, 14 (3-4), 139-173, doi:10.1016/J.OCEMOD.2006.03.006
67. O. B. Fringer, J. C. McWilliams, and R. L. Street, 2006, "A new hybrid model for coastal simulations", Oceanography, 19 (1), 46-59, doi: 10.5670/oceanog.2006.91
68. **S. K. Venayagamoorthy** and O. B. Fringer, 2005, "Nonhydrostatic and nonlinear contributions to the energy flux budget of nonlinear internal waves", Geophysical Research Letters, 32, L15603. doi:10.1029/2005GL023432
69. O. B. Fringer, S. W. Armfield, and R. L. Street, 2005, "Reducing numerical diffusion in interfacial gravity wave simulations", International Journal for Numerical Methods in Fluids, 49 (3), 301-329. doi:10.1002/fld.993
70. O. B. Fringer and R. L. Street, 2003, "The dynamics of breaking progressive interfacial waves", Journal of Fluid Mechanics, 494, 319-353. doi:10.1017/S0022112003006189
71. O. B. Fringer and D. D. Holm, 2001, "Integrable vs. nonintegrable geodesic soliton behavior", Physica D., 150 (3-4), 237-263. doi:10.1016/S0167-2789(00)00215-3

Refereed Conference/Symposia Proceedings

1. **B. Wang**, O. B. Fringer, and M. T. Stacey, 2012, “Interpreting the mixing efficiency from two-equation turbulence closure models”, Proceedings of the 3rd International Symposium on Shallow Flows, Iowa, USA.
2. **V. P. Chua**, and O. B. Fringer, 2012, "Impact of tidal dispersion and time scales on numerical diffusion in unstructured-grid estuarine modeling", Proceedings of the 3rd International Symposium on Shallow Flows, Iowa, USA.
3. *M. D. Rayson*, N. L. Jones, G. N. Ivey, and O. B. Fringer, 2011, “Internal hydraulic jump formation in a deep water, continuously-stratified, unsteady channel flow”, 7th International Symposium on Stratified Flows, Rome.
4. O. B. Fringer and **B. Wang**, 2010, "Analysis of stratified flow and separation over complex bathymetry in a field-scale estuarine model ", Proceedings of the 2010 DoD HPCMP Users Group Conference, IEEE Computer Society, 171-176, (invited), Schaumburg, IL, USA, doi:10.1109/HPCMP-UGC.2010.14
5. *S. K. Venayagamoorthy*, O. B. Fringer, J. R. Koseff, and R. L. Naylor, 2009, "Simulations of aquaculture dissolved waste transport in near-coastal waters", Proceedings of the ASCE World Environmental and Water Resources Congress 2009: Great Rivers, 1-8. doi: 10.1061/41036(342)295, Kansas City, MO, USA.
6. R. Q. Wang, A. W. K. Law, E. E. Adams, and O. B. Fringer, 2009, “The determination of formation number for starting buoyant jet”, Proceedings of the 2nd International Symposium on Computational Mechanics (ISCM II) and 12th International Conference on Enhancement and Promotion of Computational Methods in Engineering and Science, AIP Conference Proceedings, v. 1233, 1636-1641. doi: 10.1063/1.3452156, Hong Kong.
7. R. Q. Wang, A. W. K. Law, E. E. Adams and O. B. Fringer, 2009, "Large-Eddy Simulation of Starting Buoyant Jets", Proceedings of the 33rd International Association of Hydraulic Engineering and Research (IAHR) Biennial Congress, Vancouver, Canada.
8. O. B. Fringer and **Z. Zhang**, 2008, "High-Resolution Simulations of Nonlinear Internal Gravity Waves in the South China Sea", Proceedings of the DoD HPCMP Users Group Conference, 2008, DOD HPCMP, 43-46. doi: 10.1109/DoD.HPCMP.UGC.2008.46, Seattle, WA, USA.
9. **Y.-J. Chou** and O. B. Fringer, 2007, "Modeling Sediment Suspension in High Reynolds Number Flow Using Large Eddy Simulation", Proceedings of the 5th International Symposium on Environmental Hydraulics, Tempe, AZ, USA.
10. *M. F. Barad* and O. B. Fringer, 2007, "Numerical simulations of shear instabilities in open-ocean internal gravity waves", Proceedings of the 5th International Symposium on Environmental Hydraulics, Tempe, AZ, USA.
11. *S. K. Venayagamoorthy*, O. B. Fringer, J. R. Koseff, and R. L. Naylor, 2007, "Simulations of mixing and transport of dissolved wasted discharged from an aquaculture pen", Proceedings of the 5th International Symposium on Environmental Hydraulics, Tempe, AZ, USA.

12. **B. Wang** and O. B. Fringer, 2007, "Modeling the dynamics of the Snohomish River Estuary with a finite volume, unstructured-grid parallel coastal ocean simulator", Proceedings of the 5th International Symposium on Environmental Hydraulics, Tempe, AZ, USA.
13. **Z. Zhang** and O. B. Fringer, 2006, "A Numerical Study of Nonlinear Internal Wave Generation in the Luzon Strait", Proceedings of the 6th International Symposium on Stratified Flows, pp 300-305, Perth, Australia.
14. *M. F. Barad*, O. B. Fringer, and P. Colella, 2006, "Multiscale simulations of internal gravity waves", Proceedings of the 6th International Symposium on Stratified Flows, pp 722-727, Perth, Australia.
15. **S. M. Jachec**, O. B. Fringer, M. Gerritsen, and R. L. Street, 2006, "The Three-Dimensional, Time-Dependent Nature of Internal Waves Entering Monterey Submarine Canyon", Proceedings of the 6th International Symposium on Stratified Flows, pp 294-299, Perth, Australia.
16. **S. K. Venayagamoorthy** and O. B. Fringer, 2006, "The dynamics of breaking internal gravity waves over a shelf break", Proceedings of the 6th International Symposium on Stratified Flows, pp 384-389, Perth, Australia.
17. O. B. Fringer, E. S. Gross, M. Meuleners, and G. N. Ivey, 2006. "Coupled ROMS-SUNTANS simulations of highly nonlinear internal gravity waves on the Australian northwest shelf", Proceedings of the 6th International Symposium on Stratified Flows, pp 533-538, Perth, Australia.
18. **S. M. Jachec**, O. B. Fringer, M. Gerritsen, and R. L. Street, 2006. "Effects of Grid Resolution on the Simulation of Internal Tides", Proceedings of the 16th International Offshore and Polar Engineering Conference, v. III, pp 432-438, San Francisco, CA, USA.
19. **D. Kang** and O. B. Fringer, 2006. "Efficient Computation of the Nonhydrostatic Pressure", Proceedings of the 16th International Offshore and Polar Engineering Conference, v. III, pp 414-419, San Francisco, CA, USA.
20. **S. K. Venayagamoorthy** and O. B. Fringer, 2006. "Internal wave energetics on a shelf break", Proceedings of the 16th International Offshore and Polar Engineering Conference, v. III, pp 473-480, San Francisco, CA, USA.
21. **Y. Chou** and O. B. Fringer, 2005, "An unstructured immersed boundary method for simulation of flow over complex topography", Proceedings of the 9th International Conference on Estuarine and Coastal Modeling, pp. 568-584. doi: 10.1061/40876(209)33, Charleston, SC, USA.
22. **D. Kang** and O. B. Fringer, 2005, "Time accuracy for pressure methods for nonhydrostatic free-surface flows", Proceedings of the 9th International Conference on Estuarine and Coastal Modeling, pp. 419-433. doi: 10.1061/40876(209)24, Charlston, SC, USA.
23. **S. K. Venayagamoorthy** and O. B. Fringer, 2004, "Energy partitioning in breaking internal waves on slopes", In: Environmental Hydraulics and Sustainable Water Management, Proceedings of the 4th International Symposium on Environmental Hydraulics and 14th Congress of Asia and Pacific Division, International Association of Hydraulic Engineering

and Research, 15-18 December 2004, Hong Kong, v. I, Edited by J.H.W. Lee, K.M. Lam, pp. 1051-1056.

24. O. B. Fringer, M. Gerritsen, and R. L. Street, 2004, "Internal waves in Monterey Bay: An application of SUNTANS", In: Environmental Hydraulics and Sustainable Water Management, Proceedings of the 4th International Symposium on Environmental Hydraulics and 14th Congress of Asia and Pacific Division, International Association of Hydraulic Engineering and Research, 15-18 December 2004, Hong Kong, v. I, Edited by J.H.W. Lee, K.M. Lam, pp. 67-75 (invited).
25. O. B. Fringer, S. W. Armfield, and R. L. Street, 2003, "A nonstaggered curvilinear grid pressure correction method applied to interfacial waves", Proceedings of the 2nd International Conference on Heat transfer, Fluid Mechanics, and Thermodynamics (HEFAT), Victoria Falls, Zambia.
26. O. B. Fringer, S. W. Armfield, and R. L. Street, 2000, "Direct numerical simulation of unstable finite amplitude progressive interfacial waves", Proceedings of the 5th International Symposium on Stratified Flows, pp. 749-754, Vancouver, Canada.
27. O. B. Fringer and R. L. Street, 2001, "The dynamics of breaking progressive interfacial waves", Proceedings of the 3rd International Symposium on Environmental Hydraulics, Tempe, AZ, USA.

Non-refereed Conference/Symposia Proceedings

1. **G. T. C. Gil** and O. B. Fringer, 2016, "Particle transport due to trapped cores", 8th International Symposium on Stratified Flows, San Diego, CA.
2. **R. S. Arthur,** S. K. Venayagamoorthy, J. R. Koseff, and O. B. Fringer, 2016, "Quantification of highly unsteady and inhomogeneous stratified turbulence in breaking internal waves on slopes", 8th International Symposium on Stratified Flows, San Diego, CA.
3. O. B. Fringer, 2009, "Towards nonhydrostatic ocean modeling with large-eddy simulation", Oceanography in 2025: Proceedings of a Workshop, pp 81-83, The National Academies Press.

Edited Works in Print or in Press

1. A. Desbonnet, Ed., 2008, Ecosystem-based Estuary Management: A Case Study of Narragansett Bay, Chapter 14, "Circulation and pollutant transport dynamics in Narragansett Bay", by J. Craig Swanson & Malcolm L. Spaulding, Springer Series on Environmental Management, New York: Springer.

Presentations

Invited Plenary Talks and Distinguished Lectures

1. O. B. Fringer and **Y. Zhang**, 2016, "Subgrid hydrodynamics and sediment transport modeling on unstructured grids", 15th International workshop on Multi-scale (Un)-structured mesh numerical Modeling for coastal, shelf, and global ocean dynamics, September 27-29, Toulouse, France (keynote).
2. O. B. Fringer, 2016, "Numerical simulations to understand the dynamics, energetics, and mixing of breaking internal gravity waves", B'Waves 2016, June 13-17, Bergen, Norway (keynote).
3. O. B. Fringer and **R. S. Arthur**, 2016, "Transport and mixing due to breaking internal gravity waves on slopes", European Congress on Computational Methods in Applied Sciences and Engineering, June 5-10, Crete, Greece (keynote).
4. **B. Wang**, O. B. Fringer and M. Gerritsen, 2007, "Numerical techniques in a parallel, unstructured-grid, finite-volume coastal ocean simulation tool", Ninth U.S. National Congress on Computational Mechanics, San Francisco, CA (keynote).
5. O. B. Fringer, 2004, "Fluids, Math, Computers, and the Environment", Southern California Applied Mathematics Symposium (SOCAMS), Claremont, CA (keynote).

Other Invited Presentations

1. O. B. Fringer, **K.R. Scheu**, D. A. Fong, and S. G. Monismith, 2017, "Modeling intrusive, sediment-laden gravity currents in a rotationally-influenced lake", IUTAM/AMERIMECH SYMPOSIUM on the Dynamics of gravity currents, September 25-27, Santa Barbara, CA.
2. O. B. Fringer and **Y. Zhang**, 2016, "Subgrid bathymetry for seamless 1d, 2d, and 3d hydrodynamics and sediment transport modeling in SUNTANS", California Water and Environmental Modeling Forum, April 11-13, Folsom, CA.
3. **Y. Zhang**, O. Fringer, I. Huang, D. Fong, and S. Monismith, 2015, "Sediment transport modeling in a San Francisco Bay salt marsh", California Water and Environmental Modeling Forum, March 11, Folsom, CA.
4. O. B. Fringer, 2015, "Three-dimensional coupled wind-wave and cohesive sediment transport modeling in South San Francisco Bay", 2015 SIAM Conference on Computational Science and Engineering, March 13-18, Salt Lake City, UT.
5. **Y. Zhang**, O. B. Fringer, I. Huang, D. A. Fong, and S. G. Monismith, 2015, "The Impact of Vegetation and Culverts on Sediment Transport in a San Francisco Bay Salt Marsh", SIAM Conference on Mathematical and Computational Issues in the Geosciences, June 29-July 2, Stanford, CA.
6. *M. Rayson*, E. Gross, and O. B. Fringer, 2015, "Challenges in three-dimensional hydrodynamic modelling of the shallow bays and estuaries along the Gulf of Mexico coast", SIAM Conference on Mathematical and Computational Issues in the Geosciences, June 29-July 2, Stanford, CA.

7. O. B. Fringer and **R. S. Arthur**, 2015, "Direct numerical simulation of transport and mixing in breaking internal waves on slopes", 13th U.S. National Congress on Computational Mechanics, July 27-30, San Diego, CA.
8. **Y. Zhang** and O. B. Fringer, 2015, "1D, 2D, and 3D Unstructured-grid modeling of sediment transport in a salt-marsh estuary", 13th U.S. National Congress on Computational Mechanics, July 27-30, San Diego, CA.
9. O. B. Fringer, S. Vitousek, and **Y. Zhang**, 2015, "A model to simulate nonhydrostatic internal gravity waves in the ocean", AGU Fall Meeting Abstract NG13B-07, December 14, San Francisco, CA.
10. O. B. Fringer, 2013, "Modeling internal wave-induced transport in the coastal ocean", Workshop on Modeling in Support of Coastal Hypoxia, Acidification and Nutrient Management in the California Current, December 10-11, Costa Mesa, California.
11. O. B. Fringer, 2013, "Towards large-eddy simulation of internal waves in the coastal ocean", Gordon Research Conference on Coastal Ocean Circulation, Biddeford, Maine.
12. O. B. Fringer and **P. J. Wolfram**, 2013, "Dealing with divergence errors and noise in C-grid finite-volume hydrodynamic models", Advances on Computational Mechanics: A Conference Celebrating the 70th Birthday of Thomas J. R. Hughes, San Diego.
13. O. B. Fringer, **S. Vitousek**, and **P. J. Wolfram**, 2012, "Finite-volume, nonhydrostatic ocean modeling on unstructured grids", 1st International Conference on Frontiers in Computational Physics: Modeling the Earth System, Boulder.
14. R.C. Holleman, E.S. Gross, L.J. MacVean, M.T. Stacey, and O.B. Fringer, 2012, "Modelling Hydrodynamics, Sediment Transport and Provenance in the South San Francisco Bay Salt Ponds", AGU Fall Meeting, San Francisco, CA, Abstract OS23D-04.
15. O. B. Fringer, 2011, "Grid resolution requirements and computational overhead in nonhydrostatic coastal ocean modeling", Minisymposium "Recent advances in coastal ocean modeling", SIAM Conference on Mathematical & Computational Issues in the Geosciences, Long Beach, CA.
16. O. B. Fringer and **B. Wang**, 2010, "High-resolution numerical simulation of surface salinity variability over an abrupt sill in a salt-wedge estuary", American Geophysical Union (AGU) Fall Meeting, San Francisco, CA.
17. O. B. Fringer, 2010, "Three-Dimensional Modeling of Sediment Dynamics in San Francisco Bay Using the SUNTANS Model", The 6th Biennial Bay-Delta Science Conference, Sacramento, CA..
18. O. B. Fringer and **B. Wang**, 2010, "Analysis of Stratified Flow and Separation Over Complex Bathymetry in a Field-Scale Estuarine Model", DOD HPCMP Users Group Conference, Shaumburg, IL
19. O. B. Fringer and **B. Wang**, 2010, "Challenges in high-resolution simulations of macrotidal estuaries", American Geophysical Union (AGU) Ocean Sciences Meeting, Eos Trans. AGU, 91(26), Ocean Sci. Meet. Suppl., Abstract IT25H-04, Portland, OR.

20. **D. Kang** and O. B. Fringer, 2010, "The energetics of barotropic and baroclinic tides in the Monterey Bay area", American Geophysical Union (AGU) Ocean Sciences Meeting, Eos Trans. AGU, 91(26), Ocean Sci. Meet. Suppl., Abstract PO31C-03, Portland, OR.
21. **Z. Zhang**, O. B. Fringer, and S. R. Ramp, 2010, "Determining the phase in the tide at which internal waves are generated over ridges", American Geophysical Union (AGU) Ocean Sciences Meeting, Eos Trans. AGU, 91(26), Ocean Sci. Meet. Suppl., Abstract PO43C-02, Portland, OR.
22. O. B. Fringer, 2009, "Multi-scale numerical simulation of internal waves in the ocean", 4th Warnemunde Turbulence Days Workshop, Warnemunde, Germany.
23. O. B. Fringer, *S. K. Venayagamoorthy*, and J. R. Koseff, 2009, "Characteristics of waste plumes from aquaculture pens in the marine environment", AAAS Annual Meeting, Chicago, IL.
24. O. B. Fringer, 2009, "High-resolution 3D hydrodynamics and sediment transport modeling of San Francisco Bay", Interagency Ecological Program (IEP) "Physical Modeling and Fish Management" workshop, Sacramento, CA.
25. **B. Wang** and O. B. Fringer, 2008, "High-resolution simulations of a salinity front interacting with complex geometry and intertidal mudflats", American Geophysical Union (AGU) Ocean Sciences Meeting, Orlando, FL.
26. O. B. Fringer, 2007, "Multiscale simulations of internal waves and other coastal processes", Gordon Research Conference on Coastal Ocean Modeling, New London, NH.
27. **Z. Zhang** and O. B. Fringer, 2007, "Nonhydrostatic effects of nonlinear internal wave propagation in the South China Sea", American Geophysical Union (AGU) Joint Assembly Meeting, Eos Trans. AGU, 88 (23), Jt. Assem. Suppl., Abstract OS41A-06, Acapulco, Mexico.
28. O. B. Fringer, 2006, "Parallel performance of a nonhydrostatic, unstructured-grid coastal ocean model", National Science Foundation Petascale Computing and the Geosciences Workshop, La Jolla, CA.

Contributed Conference Presentations

1. **K. Nelson** and O. B. Fringer, 2018, “Unexpected fluid and sediment transport dynamics in shallow-water wave and current driven environments”, AGU Ocean Sciences Meeting, February 11-16, Portland, OR.
2. **Y. Zhang**, S. Vitousek, and O. B. Fringer, 2018, “An adaptive vertical coordinate for unstructured-grid, nonhydrostatic ocean modeling”, AGU Ocean Sciences Meeting, February 11-16, Portland, OR.
3. O. B. Fringer and **R. S. Arthur**, 2018, “Transport and dispersion due to breaking internal gravity waves on slopes”, AGU Ocean Sciences Meeting, February 11-16, Portland, OR.
4. **E. Mayer** and O. B. Fringer, 2018, “The lee-wave Froude number and its intuition”, AGU Ocean Sciences Meeting, February 11-16, Portland, OR.

5. **J. Adelson**, R. Holleman, and O. B. Fringer, 2018, “Observations of Suspended Sediment Dynamics in San Francisco Bay using Landsat 7 Imagery”, AGU Ocean Sciences Meeting, February 11-16, Portland, OR.
6. *J. Rogers*, D. Ko, and O. B. Fringer, 2018, “A framework for seamless one-way nesting of internal wave-resolving ocean models”, AGU Ocean Sciences Meeting, February 11-16, Portland, OR.
7. **K. Scheu**, O. B. Fringer, D. Fong, and S. G. Monismith, 2018, “The role of lateral boundaries in sediment transport due to river plumes in rotational, stratified environments”, AGU Ocean Sciences Meeting, February 11-16, Portland, OR.
8. **S. White, J. Adelson**, D. Freyberg, and O. B. Fringer, 2018, “Estimating Sediment Budget in South San Francisco Bay from Limited Streamflow Data”, AGU Ocean Sciences Meeting, February 11-16, Portland, OR.
9. E. Masunaga, O. B. Fringer, H. Yamazaki, R. S. Arthur, and K. Wada, 2018, “Numerical simulations and observations of nonlinear internal tides in shallow coastal regions”, AGU Ocean Sciences Meeting, February 11-16, Portland, OR.
10. O. B. Fringer, **R. S. Arthur**, S. K. Venayagamoorthy, and J. R. Koseff, 2017, “The effect of different methods to compute N on estimates of mixing in stratified flows”, 70th Annual Meeting of the APS Division of Fluid Dynamics, November 19-21, Denver, CO.
11. **Y. Zhang**, S. Vitousek, and O.B. Fringer, 2017, “A hybrid vertical coordinate for unstructured-grid, nonhydrostatic ocean modeling”, The 16th International workshop on Multi-scale (Un)-structured mesh numerical Modeling for coastal, shelf, and global ocean dynamics, August 29-September 1, Stanford, CA.
12. B. Wang, L. Cao, O.B. Fringer, F. Micheli, and R. Naylor, 2017, “Model study of the effects of intensive aquaculture on residence time and nutrient transport in a coastal embayment”, The 16th International workshop on Multi-scale (Un)-structured mesh numerical Modeling for coastal, shelf, and global ocean dynamics, August 29-September 1, Stanford, CA.
13. **W. Chen**, S. L. Billington, and O. B. Fringer, 2017, “An unstructured-grid, cut-cell model for scour simulation”, The 16th International workshop on Multi-scale (Un)-structured mesh numerical Modeling for coastal, shelf, and global ocean dynamics, August 29-September 1, Stanford, CA.
14. E. Masunaga, O.B. Fringer, H. Yamazaki, 2017, “Nonlinear internal wave dynamics and sediment transport processes investigated with the SUNTANS model”, The 16th International workshop on Multi-scale (Un)-structured mesh numerical Modeling for coastal, shelf, and global ocean dynamics, August 29-September 1, Stanford, CA.
15. **J. H. Adelson** and O. B. Fringer, 2017, “Remote Sensing of Sediment Dynamics and Critical Shear Stress in San Francisco Bay”, Gordon Research Conference on Coastal Ocean Dynamics, June 11-16, Biddeford, ME.
16. **E. T. Mayer** and O. B. Fringer, 2017, “The dynamics of unmapped bathymetry: Lee waves”, Gordon Research Conference on Coastal Ocean Dynamics, June 11-16, Biddeford, ME.

17. E. Masunaga, G. Auger, M. Rayson, O. Fringer, Y. Uchiyama, and H. Yamazaki, 2017, "Numerical simulations of the interaction between internal waves and the Kuroshio Current over the Izu-Ogasawara Ridge", AOGS 14th Annual Meeting, August 6-11, Singapore.
18. **K. Nelson** and O. B. Fringer, 2016, "Understanding the effects of sediment stratification in shallow wave and current driven environments", AGU Fall Meeting, December 12-16, San Francisco, CA.
19. **J. Adelson**, N. Kau, and O. B. Fringer, 2016, "Remote sensing to infer surface SPM in San Francisco Bay", 9th Biennial Bay-Delta Science Conference, November 15-17, Sacramento, CA.
20. **J. Adelson**, R. James, V. Chirayath, and O.B. Fringer, 2016, "Calibration and Testing of an Active Multispectral Instrument for Remote Sensing Suspended Particulate Matter", Ocean Optics Conference, November 8-12, Victoria, BC, Canada.
21. **K. Nelson** and O. B. Fringer, 2016, "Reducing spin-up time for DNS and LES of turbulent channel flow", 69th Annual Meeting of the APS Division of Fluid Dynamics, 61 (20), Abstract KP1.00134, November 20-22, Portland, OR.
22. E. Masunaga, O. B. Fringer, and H. Yamazaki, 2016, "Generation mechanisms and energetics of internal waves around an island", PO33B-05, AGU Ocean Sciences Meeting Abstract MG14A-1901, February 21-26, Portland, Oregon
23. **R. S. Arthur**, J. R. Koseff, and O. B. Fringer, 2016, "Local vs. bulk measures of the mixing efficiency in breaking internal waves on slopes", AGU Ocean Sciences Meeting Abstract PO24E-2998, February 21-26, Portland, Oregon.
24. **K. R. Scheu**, D. A. Fong, S. G. Monismith, and O. B. Fringer, 2016, "Sedimentation dynamics of a sediment-laden river intrusions in a large alpine lake", AGU Ocean Sciences Meeting Abstract MG14A-1901, February 21-26, Portland, Oregon.
25. S. Y. Litvin, J. M. Beers, C. B. Woodson, P. Leary, O. B. Fringer, J. A. Goldbogen, F. Micheli, S. G. Monismith, G. N. Somero, 2016, "Quantifying physiological, behavioral and ecological consequences of hypoxic events in kelp forest", AGU Ocean Sciences Meeting Abstract ME24E-0759, February 21-26, Portland, Oregon.
26. *M. D. Rayson*, E. S. Gross, and O. B. Fringer, 2015, "Physical processes controlling tracer exchange at the mouth of Galveston Bay", Gulf of Mexico Oil Spill and Ecosystem Science Conference, February 16-19, Houston, TX.
27. **R. S. Arthur** and O. B. Fringer, 2015, "Transport by breaking internal waves on slopes", Gordon Research Conference on Coastal Ocean Modeling, June 7-12, Biddeford, ME.
28. **K. Nelson**, O. B. Fringer, and Y.J. Chou, 2015, "A three-dimensional sediment transport model and its application for studying shoal and channel sediment dynamics", Gordon Research Conference on Coastal Ocean Modeling, June 7-12, Biddeford, ME.
29. *M. Rayson*, E. Gross, R. Hetland, and O. Fringer, 2015, "Characterizing and modelling salinity variability in an estuary with transient river forcing", Gordon Research Conference on Coastal Ocean Modeling, June 7-12, Biddeford, ME.

30. **K. Scheu**, D. Fong, S. Monismith, and O. Fringer, 2015, “Modeling sedimentation dynamics of a sediment-laden river plume in a large alpine lake”, Gordon Research Conference on Coastal Ocean Modeling, June 7-12, Biddeford, ME.
31. **Y. Zhang** and O. B. Fringer, 2015, “New developments and applications of the parallel finite-volume unstructured-grid SUNTANS model for sediment transport within estuarine marshes”, Gordon Research Conference on Coastal Ocean Modeling, June 7-12, Biddeford, ME.
32. O. B. Fringer, *M. D. Rayson*, and P. J. Wolfram, 2015, “Are unstructured grids needed? Comparison of the accuracy of finite-volume unstructured to curvilinear and Cartesian grid ocean models”, 14th International workshop on Multi-scale (Un)-structured mesh numerical Modeling for coastal, shelf, and global ocean dynamics, September 28-30, Portland, OR.
33. O. B. Fringer and **Y. Zhang**, 2015, “Subgrid bathymetry for hydrodynamics and sediment transport in SUNTANS”, 14th International workshop on Multi-scale (Un)-structured mesh numerical Modeling for coastal, shelf, and global ocean dynamics, September 28-30, Portland, OR.
34. L. Zaninetta and O. B. Fringer, 2014, “New Ways to Assess Natural Recovery of Sediments in Lake Maggiore, Italy”, 30th Annual International Conference on Soils, Sediments, Water, and Energy, October 20-23, Amherst, MA.
35. **R.S. Arthur** and O. B. Fringer, 2014, “Turbulent dynamics of breaking internal gravity waves on slopes”, 67th Annual Meeting of the APS Division of Fluid Dynamics, 59 (20), Abstract BAPS.2014.DFD.R11.1, November 23-25, San Francisco, CA.
36. O. B. Fringer, **P. Wolfram**, N. Monsen, K. Gleichauf, D. Fong, and S. G. Monismith, 2014, “Comparison of mixing at a junction computed with two- and three-dimensional models to the simple flow-weighting scheme used in one-dimensional models”, 8th Biennial Bay-Delta Science Conference, October 28-30, Sacramento, CA.
37. M. van der Wegen, L. Lucas, N. Knowles, D. Senn, B. Jaffe, E. Elias, P. Barnard, M. Stacey, O. Fringer, E. Gross, T. Fregoso, R.C. Martyr, F. Achete, E. Melger, F. Baart, H. Los, T. Troost, J. Smits, D. Roelvink, 2014, “Building a Public Community around the D3D-FM San Francisco Bay-Delta Model”, 8th Biennial Bay-Delta Science Conference, October 28-30, Sacramento, CA.
38. *M. D. Rayson*, E. S. Gross, R. D. Hetland, O. B. Fringer, 2014, “Tracer age as a diagnostic for understanding the relationship between surface and boundary forcing and estuarine circulation”, Poster 3-63, Gulf of Mexico Oil Spill & Ecosystem Science Conference, January 26-28, Mobile, AL.
39. **R. S. Arthur** and O. B. Fringer, 2014, "Transport and mixing by breaking internal waves on slopes", 61st Annual Eastern Pacific Ocean Conference (EPOC). September 17-20, Mt. Hood, OR.
40. **R. S. Arthur** and O. B. Fringer, 2014, “Cross-stream variability in breaking internal waves on slopes”, Nonlinear effects in internal waves conference, June 9-12, Cornell, NY.

41. K. G. Gleichauf, **P. Wolfram**, N. Monsen, O. Fringer, and S. Monismith, 2014, “Dispersion mechanisms in a tidal river junction in the Sacremento-San Joaquin Delta, CA”, AGU Ocean Sciences Meeting Abstract 14592, February 23-28, Honolulu, HI.
42. **R. S. Arthur** and O. B. Fringer, 2014, “The three-dimensional structure and energetics of breaking internal waves on slopes”, AGU Ocean Sciences Meeting Abstract 13316, February 23-28, Honolulu, HI.
43. N. L. Jones, C. E. Bluteau, *M. D. Rayson*, O. B. Fringer, and G. N. Ivey, 2014, “Internal tide mixing on the Australian Northwest continental shelf and slope”, AGU Ocean Sciences Meeting Abstract 15994, February 23-28, Honolulu, HI.
44. O. B. Fringer, *B. Wang*, N L. Jones, and G. N. Ivey, 2014, “Numerical modeling of nonlinear and nonhydrostatic internal waves on the Australian North West shelf”, AGU Ocean Sciences Meeting Abstract 16541, February 23-28, Honolulu, HI.
45. *M. D. Rayson*, O. B. Fringer, E. S. Gross, and R. D. Hetland, 2014, “Application of a nested, unstructured mesh hydrodynamic model to a bay in the Gulf of Mexico”, AGU Ocean Sciences Meeting Abstract 16922, February 23-28, Honolulu, HI.
46. **K. Scheu**, D. Fong, S. Monismith, and O. Fringer, 2014, “Seasonal variability of sediment deposition into a large alpine lake”, AGU Ocean Sciences Meeting Abstract 17645, February 23-28, Honolulu, HI.
47. N. Tahvildari, T. Peacock, and O. B. Fringer, 2014, “A parametric study of nonlinear and nonhydrostatic effects on internal tide generation over a submerged ridge”, AGU Ocean Sciences Meeting Abstract 16837, February 23-28, Honolulu, HI.
48. **S. Vitousek** and O. B. Fringer, 2014, “A nonhydrostatic isopycnal-coordinate ocean model”, AGU Ocean Sciences Meeting Abstract 15863, February 23-28, Honolulu, HI.
49. **R. S. Arthur** and O. B. Fringer, 2013, “Dissipation and mixing in breaking internal gravity waves on slopes”, Gordon Research Conference on Coastal Ocean Circulation, Biddeford, Maine.
50. N. E. Monsen, **P. Wolfram**, K. Gleichauf, O. Fringer, and S. G. Monismith, 2013, “Development of a SUNTANS model for the Sacramento-San Joaquin Delta”, 2013 California Water and Environmental Modeling Forum (CWEMF) Annual Meeting, April 22-24, Folsom, California.
51. *M. Rayson*, E. Gross, and O. B. Fringer, 2013, “Residual circulation in a shallow, micro-tidal estuary: Galveston Bay, TX”, Gordon Research Conference on Coastal Ocean Circulation, June 9-14, Biddeford, Maine.
52. *M. Rayson*, E. S. Gross, and O. B. Fringer, 2013, “Age as a diagnostic for understanding the link between surface and boundary forcing and estuarine circulation”, The 12th International workshop on Multi-scale (Un)-structured mesh numerical Modeling for coastal, shelf, and global ocean dynamics, September 16-19, Austin, Texas.
53. *M. Rayson*, E. S. Gross, and O. B. Fringer, 2013, “Development of a high-resolution, three-dimensional hydrodynamic model of Galveston Bay”, Gulf of Mexico Oil Spill and Ecosystem Science Conference, January 21-23, New Orleans, Louisiana.

54. **K. R. Scheu,** O. B. Fringer, S. G. Monismith, and D. A. Fong, 2013, “Sediment transport due to river inflows into large alpine lakes”, KITP Conference: Particle-Laden Flows in Nature, December 16-19, U. C. Santa Barbara.
55. **K. R. Scheu,** S. G. Monismith, D. A. Fong, and O. B. Fringer, 2013, “Seasonal variability of sediment and contaminant transport in Lake Maggiore, Italy”, 16th Workshop on Physical Processes in Natural Waters, July 8-11, Queensland, Australia (awarded best presentation).
56. **S. Vitousek** and O. B. Fringer, 2013, “A Nonhydrostatic Isopycnal Model for the Simulation of Internal Gravity Waves”, Gordon Research Conference on Coastal Ocean Circulation, June 9-14, Biddeford, Maine.
57. **P. Wolfram,** N. Monsen, K. Gleichauf, O. Fringer, and S. Monismith, 2013, **“**Tidal dispersion and the impact of small-scale flow features in channel junctions”, Gordon Research Conference on Coastal Ocean Circulation, Biddeford, Maine.
58. **P. Wolfram,** N. E. Monsen, K. Gleichauf, O. Fringer, and S. G. Monismith, 2013, “Computing Secondary Flows in the Delta: The Problem of Noise on Unstructured C-grids”, California Water and Environmental Modeling Forum (CWEMF) Annual Meeting, April 22-24, Folsom, California.
59. **Y. Zhang** and O. B. Fringer, 2013, “New developments for the parallel finite-volume unstructured-grid SUNTANS model”, The 12th International workshop on Multi-scale (Un)-structured mesh numerical Modeling for coastal, shelf, and global ocean dynamics, September 16-19, Austin.
60. *Y. Chou*, R. C. Holleman, S. Lee, C. Chang, O. B. Fringer, M. T. Stacey, S. G. Monismith, and J. R. Koseff, 2012, “Three-Dimensional Numerical Modeling of Sediment Suspension in San Francisco Bay”, AGU Fall Meeting, San Francisco, CA, Abstract OS21C-1767.
61. **R. S. Arthur**, R.K. Walter, C.B. Woodson, O.B. Fringer, and S.G. Monismith,2012, “Field and Numerical Investigation of Nearshore Internal Bores”, 59th Annual Eastern Pacific Ocean Conference (EPOC), September 22, 2012. Mt. Hood, OR.
62. **P. Wolfram** and O. Fringer, 2012, “Mitigating divergence-error oscillations in triangular C grids for nonlinear and nonhydrostatic flows”, Workshop on Multiscale Modelling of Coastal, Shelf and Ocean Dynamics (IMUM), Delft, Netherlands.
63. **P. Wolfram**, N. Monsen, K. Gleichauf, O. Fringer, and S. Monismith, 2012, “Characterizing the effect of small scale flow features on dispersion within channel junctions”, 7th Biennial Bay-Delta Science Conference, Sacramento, CA.
64. N. E. Monsen, **P. Wolfram**, K. Gleichauf, O. Fringer, and S. Monismith, 2012, “The Devil is in the details: why the representation of the flow field, especially at junctions, matters in order to simulate dispersion in the Delta”, 7th Biennial Bay-Delta Science Conference, Sacramento, CA.
65. **S. Koltakov,** G. Iaccarrino, and O. B. Fringer, 2012, “Inferring bottom bathymetry from free-surface flow features”, SIAM Conference on Uncertainty Quantification, Raleigh, North Carolina.

66. **V. P. Chua**, O. B. Fringer, D. A. Fong, S. G. Monismith, and J. R. Koseff, 2012, “Modeling the impact of sea-level rise on salinity intrusion in San Francisco Bay”, 2012 Ocean Sciences Meeting, Salt Lake City, Abstract 9460.
67. R. B. Zeller, J. S. Weitzman, M. E. Abbett, O. B. Fringer, and J. R. Koseff, 2012, “Seagrass blade dynamics in unidirectional, oscillatory, and combined flows”, 2012 Ocean Sciences Meeting, Salt Lake City, Abstract 9801.
68. **G. Trigo Cabrita Gil** and O. B. Fringer, 2012, “Lagrangian- and Eulerian-mean effects in progressive internal gravity waves”, 2012 Ocean Sciences Meeting, Salt Lake City, Abstract 10029.
69. **K. R. Scheu**, O. B. Fringer, S. G. Monismith, D. Lin, and R. G. Luthy, 2012, “Rotational effects on sediment and DDT transport within a large lake (Lake Maggiore, Italy)”, 2012 Ocean Sciences Meeting, Salt Lake City, Abstract 10877.
70. K. T. Gleichauf, **P. J. Wolfram,** S. G. Monismith, O. B. Fringer, N. E. Monsen, and A. M. Bayen, 2012, “Small-scale hydrodynamics in tidal river junctions in the Sacramento-San Joaquin River Delta”, 2012 Ocean Sciences Meeting, Salt Lake City, Abstract 12139.
71. **S. Vitousek** and O. B. Fringer, 2012, “Grid resolution requirements in modeling internal waves”, 2012 Ocean Sciences Meeting, Salt Lake City, Abstract 12494.
72. **B. Wang, P. J. Wolfram,** G. Zhao, and O. B. Fringer, 2011, “Reconstruction of vector fields for semi-Lagrangian advection on unstructured, staggered grids”, The 10th International Workshop on Multiscale (Un-)structured Mesh Numerical Modelling for coastal, shelf and global ocean dynamics, Bremerhaven, Germany, August 22-25.
73. R. Holleman, **V. Chua**, M. Stacey, and O. B. Fringer, 2011, “Numerical scalar diffusion on flow-aligned unstructured, finite-volume grids”, The 10th International Workshop on Multiscale (Un-)structured Mesh Numerical Modelling for coastal, shelf and global ocean dynamics, Bremerhaven, Germany, August 22-25.
74. O. B. Fringer and **S. Vitousek**, 2011, “Physical vs numerical dispersion in nonhydrostatic internal wave modeling”, Conference on Geophysical and Astrophysical Internal Waves, Les Houches, France.
75. S. Sankaranarayanan and O. B. Fringer, 2010, "Dynamics of Low-frequency fluctuations in San Francisco Bay due to upwelling", AGU Fall Meeting, San Francisco, CA, USA.
76. *Y. Chou* and O. B. Fringer, 2010, "Coupled Wave-Current Numerical Simulation of Cohesive Sediment Transport in San Francisco Bay using SUNTANS", AGU Fall Meeting, San Francisco, CA, USA.
77. **Gil, G. T. C.**, and O. B. Fringer, 2010, "On the potential for transport via internal tides in the coastal ocean", 63rd Annual Meeting of the APS Division of Fluid Dynamics, 55 (16), Long Beach, CA, USA.
78. O. B. Fringer and **Z. Zhang**, 2010, “Understanding internal wave generation in the South China Sea using three-dimensional numerical simulations”, BIRS Coordinated Mathematical Modeling of Internal Waves, Banff, Canada.

79. **B. Wang** and O. B. Fringer, 2010, "High-resolution simulations of stratified flow and separation over an abrupt sill in a shallow estuary", 9th International workshop on Multiscale (Un)-structured mesh numerical Modeling for coastal, shelf, and global ocean dynamics, MIT, Cambridge, MA, USA.
80. **V. Chua** and O. B. Fringer, 2010, "Assessing the effects of numerical diffusion in a three-dimensional unstructured-grid model of a periodically-stratified estuary", 9th International workshop on Multiscale (Un)-structured mesh numerical Modeling for coastal, shelf, and global ocean dynamics, MIT, Cambridge, MA, USA.
81. **Y. Chou** and O. B. Fringer, 2010, "Numerical simulation of combined wave-current flows over dynamic sand ripples", Eos Trans. AGU, 91(26), Ocean Sci. Meet. Suppl., Abstract PO15E-30, Portland, OR, USA.
82. **B. Wang**, O. B. Fringer, and E. S. Gross, 2010, "Understanding turbulent mixing in a partially stratified estuary using SUNTANS", Eos Trans. AGU, 91(26), Ocean Sci. Meet. Suppl., Abstract PO45I-10, Portland, OR, USA.
83. O. B. Fringer and *M. F. Barad*, 2009, "Numerical simulation of shear instabilities in interfacial gravity waves", 4th Warnemunde Turbulence Days Workshop, Warnemunde, Germany.
84. *M. Barad* and O. B. Fringer, 2009, "Large-eddy simulation of coherent flow structures in a river", DOD HPCMP Users Group Conference, San Diego, CA, USA.
85. **Y. Chou** and O. B. Fringer, 2009, "Numerical simulation of turbulence-induced sediment transport and the resulting bedform dynamics", Workshop on modeling of turbidity currents and related gravity currents, Santa Barbara, CA, USA.
86. **Y. Chou** and O. B. Fringer, 2009, "Numerical Simulation of Turbulence-Induced Bedform Initiation", 62nd Annual Meeting of the APS Division of Fluid Dynamics, 54 (19), Abstract BAPS.2009.DFD.AC.6, http://meetings.aps.org/link/BAPS.2009.DFD.AC.6, Chicago, IL, USA.
87. O. Fringer and *M. Barad*, 2009, "Numerical simulation of shear instabilities in interfacial gravity waves", 62nd Annual Meeting of the APS Division of Fluid Dynamics, 54 (19), Abstract BAPS.2009.DFD.HS.4, http://meetings.aps.org/link/BAPS.2009.DFD.HS.4, Chicago, IL, USA.
88. **Chou, Y.**, Fringer, O. B., and J. R. Lacy, 2008, "Numerical Study of Sediment Suspension over Bedforms in Combined Flows", Eos Trans. AGU, 89(53), Fall Meet. Suppl., Abstract OS21E-1204, San Francisco, CA, USA.
89. *S. K. Venayagamoorthy*, O. B. Fringer, R. Naylor, and J. R. Koseff, 2008, " Numerical simulations of aquaculture dissolved waste transport in a coastal embayment", 61st Annual Meeting of the APS Division of Fluid Dynamics, 53 (15), Abstract BAPS.2008.DFD.HV.9, http://meetings.aps.org/link/BAPS.2008.DFD.HV.9, San Antonio, TX, USA.
90. O. B. Fringer, 2008, "Nonhydrostatic effects of internal solitary-like waves and possible parameterizations for hydrostatic models", Eos Trans. AGU, 89(53), Fall Meet. Suppl., Abstract OS51F-08, San Francisco, CA, USA.

91. **Wang, B.**, and O. B. Fringer, 2008, "Nonhydrostatic effects in high-resolution estuarine simulations", Seventh International Workshop on Unstructured Grid Numerical Modelling of Coastal, Shelf and Ocean Flows, Halifax, Canada.
92. *M. F. Barad*, O. B. Fringer, and P. MacCready, 2008, "Surface Signatures Generated by one- and two-dimensional sinusoidal bathymetry", AGU Ocean Sciences Mtng., Orland, FL, USA.
93. **D. Kang** and O. B. Fringer, 2008, "Simulation of the interaction of mesoscale currents with internal tides", AGU Ocean Sciences Mtng., Orlando, FL, USA.
94. *S. K. Venayagamoorthy*, O. B. Fringer, J. R. Koseff, and R. L. Naylor, 2008, "Simulations of mixing and transport of dissolved wasted discharged from near-coastal aquaculture pens", AGU Ocean Sciences Mtng., Orlando, FL, USA.
95. **Z. Zhang** and O. B. Fringer, 2008, "Numerical simulation of the generation of nonlinear internal gravity waves in the South China Sea"", AGU Ocean Sciences Mtng., Orlando, FL, USA.
96. *S. K. Venayagamoorthy*, O. B. Fringer, J. R. Koseff, and R. L. Naylor, 2007, "Simulations of Mixing and Transport of Dissolved Waste Discharged From a Submerged Aquaculture pen", Eos Trans. AGU, 88 (23), Jt. Assem. Suppl., Abstract OS23G-02, Acapulco, Mexico.
97. O. B. Fringer, S. J. Macumber, and A. B. Boehm, 2007, "Transport due to Internal Waves in the San Pedro Bay Region", Eos Trans. AGU, 88 (23), Jt. Assem. Suppl., Abstract OS23G-04, Acapulco, Mexico.
98. **S. M. Jachec**, O. B. Fringer, M. Gerritsen, and R. L. Street, 2006, "Understanding Internal Tides within Monterey Bay: from Beams to Modes", Eos Trans. AGU, 87(52), Fall Meet. Suppl., Abstract OS13A-1542, San Francisco, CA.
99. **Z. Zhang** and O. B. Fringer, 2006, "Simulation of Nonlinear Internal Wave Generation in the Northeastern South China Sea", Eos Trans. AGU, 87(52), Fall Meet. Suppl., Abstract OS13A-1533, San Francisco, CA.
100. **B. Wang**, O. B. Fringer, and R. L. Street, 2006, "Application of an unstructured-grid, finite-volume parallel coastal ocean simulator to the Snohomish River Estuary", Proceedings of the fifth international workshop on unstructured mesh numerical modelling of coastal, shelf and ocean flows, Miami, FL, USA.
101. **S. K. Venayagamoorthy** and O. B. Fringer, 2006. " Dynamics of internal boluses across a shelf break", 59th Annual Meeting of the Division of Fluid Dynamics, American Physical Society, Abstract BAPS.2006.DFD.FG.3, http://meetings.aps.org/link/BAPS.2006.DFD.FG.3, Tampa Bay, FL, USA.
102. D. A. Fong and O. B. Fringer, 2006, "High-resolution, nonhydrostatic flow physics in shallow coastal and estuarine flows", Eos Trans. AGU, 87(36), Ocean Sci. Meet. Suppl., Abstract OS35D-11, Honolulu, HI, USA.
103. **S. K. Venayagamoorthy** and O. B. Fringer, 2006, "Dynamics of the interaction of breaking internal gravity waves with a shelf break", Eos Trans. AGU, 87(36), Ocean Sci. Meet. Suppl., Abstract OS12J-05, Honolulu, HI, USA.

104. J. Majkut and O. B. Fringer, 2006, `Modeling the Interaction of Internal Tides and Wind Stress Over the Bathymetry of Huntington Beach, CA", Eos Trans. AGU, 87(36), Ocean Sci. Meet. Suppl., Abstract OS26H-14, Honolulu, HI, USA.
105. **J. Wang**, R. L. Street, and O. B. Fringer, 2006, "Nonhydrostatic Numerical Simulation of Internal Solitary Waves in the South China Sea", Eos Trans. AGU, 87(36), Ocean Sci. Meet. Suppl., Abstract OS15A-2, Honolulu, HI, USA.
106. **S. M. Jachec**, O. B. Fringer, R. L. Street, and M. Gerritsen, 2006, "Tidally Partitioned Energetics for Monterey Bay Derived From Numerical Simulations", Eos Trans. AGU, 87(36), Ocean Sci. Meet. Suppl., Abstract OS26H-21, Honolulu, HI, USA.
107. A. E. Santoro, K. R. Arrigo, O. B. Fringer, and A. B. Boehm, 2006, "Physical Predictors of Biological Water Quality: Linking Ocean Temperature and Human Health Risk," Eos Trans. AGU, 87(36), Ocean Sci. Meet. Suppl., Abstract OS25M-15, Honolulu, HI, USA.
108. G. Ivey, M. Meuleners, O. Fringer, K. Winters, and E. Gross, 2006, "Regional Model of the Internal Tide Dynamics on the Australian North West Shelf", Eos Trans. AGU, 87(36), Ocean Sci. Meet. Suppl., Abstract OS24M-06, Honolulu, HI, USA.
109. **Z. Zhang** and O. B. Fringer, 2006, "Propagation and Interaction of Nonlinear Internal Solitary Waves in the South China Sea", Eos Trans. AGU, 87(36), Ocean Sci. Meet. Suppl., Abstract OS15A-15, Honolulu, HI, USA.
110. J. Warren, A. Boehm, O. Fringer, and J. Kose, 2006, "Recreational Beach Visitor Perceptions of Health Risk and Impact of Water-Borne Pathogens in Orange County, CA," Eos Trans. AGU, 87(36), Ocean Sci. Meet. Suppl., Abstract OS25M-04, Honolulu, HI, USA.
111. **D. Kang**, O. Fringer, M. Gerritsen, Y. Kanarska, J. C. McWilliams, A. Shchepetkin, and R. L. Street, 2006, "High-resolution Simulations of Upwelling and Internal Waves in Monterey Bay Using a Coupled ROMS-SUNTANS Multi-scale Simulation Tool", Eos Trans. AGU, 87(36), Ocean Sci. Meet. Suppl., Abstract OS36G-07, Honolulu, HI, USA.
112. **S. K. Venayagamoorthy** and O. B. Fringer, 2005. "Energetics of internal boluses on a shelf break", 58th Annual Meeting of the Division of Fluid Dynamics, American Physical Society, Abstract BAPS.2005.DFD.EN.7, http://meetings.aps.org/link/BAPS.2005.DFD.EN.7, Chicago, IL, USA.
113. **S. K. Venayagamoorthy** and O. B. Fringer, 2005. "Numerical simulations of internal gravity waves", Gallery of Fluid Motion Poster (#49), 58th Annual Meeting of the Division of Fluid Dynamics, American Physical Society, Chicago, IL, USA.
114. O. B. Fringer and **S. K. Venayagamoorthy**, 2005, "Modeling the generation and evolution of internal boluses on coastal slopes ", 2005, Workshop on turbidity currents and related gravity currents, UCSB, Santa Barbara, CA, USA.
115. **S. M. Jachec**, O. B. Fringer, M. Gerritsen, and R. L. Street, 2004, "Evolution of internal waves in Monterey Bay", Eos Trans. AGU, 85(47), Fall Meet. Suppl., Abstract OS21B-1230, San Francisco, CA, USA.

116. **S. K. Venayagamoorthy** and O. B. Fringer, 2004, "Generation and evolution of solibores on slopes", Eos Trans. AGU, 85(47), Fall Meet. Suppl., Abstract OS11A-0498, San Francisco, CA, USA.
117. **S. M. Jachec**, O. B. Fringer, M. Gerritsen, and R. L. Street, 2004, "SUNTANS on Monterey Bay", Eos. Trans. AGU, 85(17), Joint Assembly Suppl., Abstract OS33A-05, Montreal, Canada.
118. O. B. Fringer and A. B. Boehm, 2004, "Cross shelf transport induced by internal tides", ASLO/TOS Ocean Research Conference, Honolulu, HI, USA.
119. O. B. Fringer, M. Gerritsen, **S. Jachec**, and R. L. Street, 2002, "A new nonhydrostatic parallel coastal ocean model," Eos Transactions, AGU, 83(47): Abstract OS11C-0238, San Francisco, CA, USA.
120. O. B. Fringer, C. D. Troy, J. R. Koseff, and R. L. Street, 2002, "Laboratory and numerical experiments on breaking interfacial waves", Eos. Trans. AGU, 83(4), Ocean Sciences Meet. Suppl., Abstract OS41E-68 (Best student poster award), Honolulu, HI, USA.
121. O. B. Fringer and R. L. Street, 2001, "The dynamics of breaking progressive interfacial waves",3rd International Symposium on Environmental Hydraulics, Tempe, AZ, USA.
122. O. B. Fringer and R. L. Street. 1999. "Nonhydrostatic effects of breaking interfacial waves on a sloping boundary," 5th Workshop on Numerical Modeling of Atmospheric, Surface, and Groundwater Flows, Trento, Italy.
123. O. B. Fringer and D. D. Holm. 1998. "Integrable vs nonintegrable geodesic soliton behavior,"IGPP/NPACIWorkshop on Accurate Simulation and Modeling of Physical Systems, (Best student poster award), La Jolla, CA, USA.
124. C. J. Mikolaijczak, M. J.Wornat, F. L. Dryer, O. B. Fringer, and T. J. Held. 1996. "A flow reactor study of 1-Methylnaphthalene pyrolysis using a new condensed-species sampling probe," ESCI Fall Technical Meeting, Hilton Head, SC, USA.
125. C. J. Mikolajczak, O. B. Fringer, T. J. Held, M. J. Wornat, and F. L. Dryer. 1996. "A new condensed species sampling probe for flow reactor studies of polycyclic aromatic compounds," 26th International Symposium on Combustion, Naples, Italy.

Former Ph.D. Students (in order of graduation year)

1. Kurt Nelson, 2018, Thesis: "Simulating sediment dynamics in shallow-water wave- and current-driven environments”
2. Yun Zhang, 2017, Thesis: "Numerical modeling for hydrodynamics and suspended sediment transport in estuarine marshes"
3. Gonçalo Gil, 2017, Thesis: "Mass transport and shear-flow dispersion due to nonlinear internal gravity waves"
4. Kara Scheu, 2016, Thesis: “Sediment transport due to river plumes in stratified, rotationally-influenced lakes”
5. Robert Arthur, 2015, Thesis: "Numerical investigation of breaking internal waves on slopes: Dynamics, energetics, and transport"

6. Sean Vitousek, 2014, Thesis: "Towards internal wave resolving simulations of the ocean"
7. Phillip Wolfram, 2014, Thesis: "Secondary flows and dispersion in channel junctions"
8. Sergey Koltakov, 2013, Thesis: "Bathymetry inference from free-surface flow features using large-eddy simulation"
9. Bing Wang, 2012, Thesis: "Multiscale numerical simulations of a complex macrotidal tidal-river estuary"
10. Vivien Chua, 2012, Thesis: "Three-dimensional, unstructured-grid numerical simulations of hydrodynamics and scalar transport in San Francisco Bay"
11. Dujuan Kang, 2011, Thesis: "Energetics and dynamics of internal tides in Monterey Bay using numerical simulations"
12. Zhonghua Zhang, 2010, Thesis: "Numerical simulations of nonlinear internal waves in the South China Sea"
13. Yi-Ju Chou, 2009, Thesis: "Numerical study of sand ripple dynamics in turbulent flows"
14. Sheng Chen, 2009, Thesis: "Adaptive error estimators for electromagnetic field solvers"
15. Steven Jachec, 2007, Thesis: "Understanding the evolution and energetics of internal tides within Monterey Bay via numerical simulations"
16. Karan Venayagamoorthy, 2006, Thesis: "Energetics and dynamics of internal waves on a shelf break using numerical simulations"

APPENDIX A-3

The **tidal period (PERIOD)** must be supplied; in most cases it is 12.4 hours, but in some locations it may vary slightly. The **maximum tidal velocity (UAmax)** for the location must be specified; this can usually be taken as the average of the absolute values of the two actual maxima, independent of their direction. A CORMIX design case consists then of an instantaneous ambient condition, before, at or after one of the two slack tides. Hence, the analyst must specify the **time** (in hours) **before, at, or after slack** that defines the design condition, followed by the actual **tidal ambient velocity (UA)** at that time. The ambient depth conditions are then those corresponding to that time.

In general, tidal simulations should be repeated for several time intervals (usually hourly or two-hourly intervals will suffice) before and after slack time to determine plume characteristics in unsteady ambient conditions.

Strongly unsteady conditions can also occur in other environments, such as in wind-induced current reversals in shallow lakes or coastal areas. In this case, any typical reversal period can be analyzed following an approach similar to the above.

4.3.4 Ambient Density Specification

Information about the density distribution in the ambient water body is very important for the correct prediction of effluent discharge plume behavior. CORMIX first inquires whether the ambient water is **fresh water** or **non-fresh** (i.e. brackish or saline). If the ambient water is fresh and above 4 °C, the system provides the option of entering ambient temperature data so that the ambient density values can be internally computed from an equation of state. This is the recommended option for specifying the density of fresh water, even though ambient temperature per se is not needed for the analysis of mixing conditions. In the case of salt water conditions, Figure 4.3 is included as a practical guide for specifying the density if "salinity values" in parts-per-thousand (ppt) are available for the water body. Typical open ocean salinities are in the range 33 - 35 ppt.

The user then specifies whether the ambient density (or temperature) can be considered as **uniform** or as **non-uniform** within the water body, and in particular within the expected plume regions. As a practical guide, vertical variation in density of less than 0.1 kg/m^3 or in temperature of less than 1 °C can be neglected. For uniform conditions, the **average ambient density** or **average temperature** must be specified.

When conditions are non-uniform, CORMIX requires that the actual measured vertical density distribution be approximated by one of three schematic stratification profile types illustrated in Figure 4.4. These are: Type A, linear density profile; Type B, two-layer system with constant densities and density jump; Type C, constant density surface layer with linear density profile in bottom layer separated by a density jump. Corresponding profile types exist for approximating a temperature distribution when it is used for specifying the density distribution.

Note: When in doubt about the specification of the ambient density values it is reasonable to first simplify as much as possible. The sensitivity of a given assumption can be explored in subsequent CORMIX simulations. Furthermore, if CORMIX indicates indeed a flow configuration (flow class) with near-field stability, additional studies with the post-processor option CORJET (see Section 6.1) can be performed to investigate *any arbitrary density distribution*.

After selecting the stratification approximation to be used, the user then enters all appropriate density (or temperature) values and **pycnocline heights (HINT)** to fully specify the profiles. The pycnocline is defined as zone or level of strong density change that separates the upper and lower layers of the water column. The program checks the density specification to insure that stable ambient stratification exists (i.e. the density at higher elevations must not exceed that at lower elevations).

Note that a dynamically correct approximation of the actua ldensity distribution should keep a balance between over-and under-estimationof the actual data similar to a best-fit in regression analysis. If simulation results indicate internal plume trapping, then it is

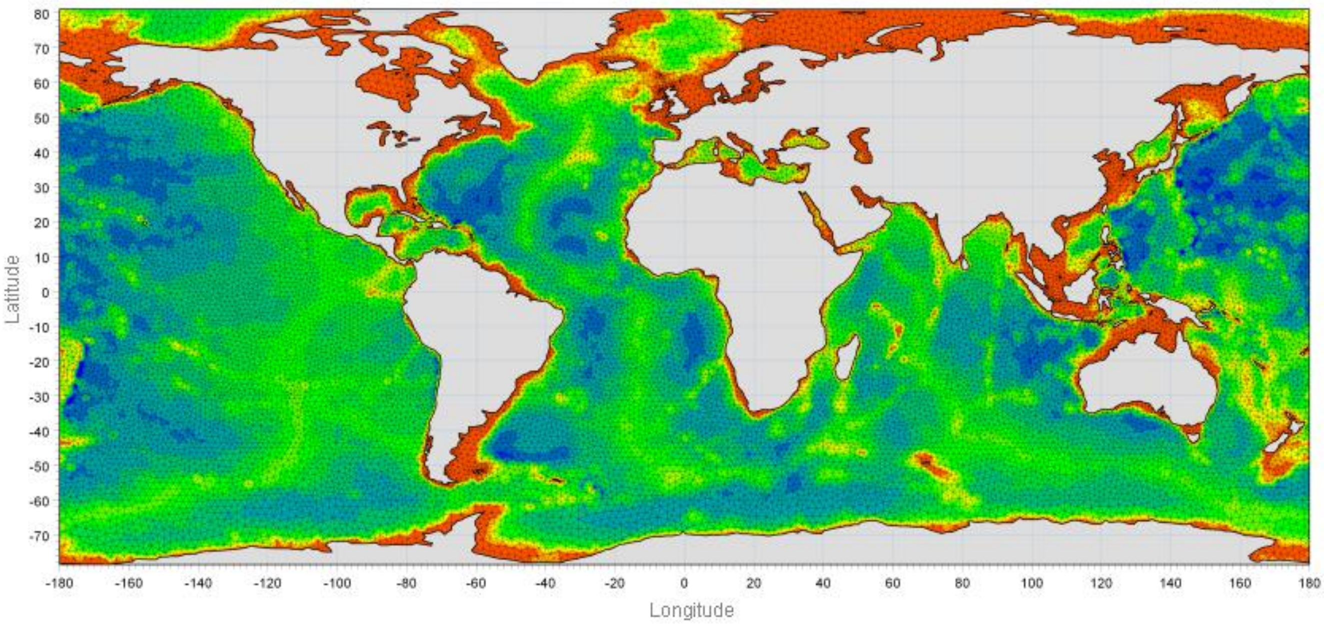

MIKE 21 & MIKE 3 FLOW MODEL FM supports both Cartesian and spherical coordinates. Spherical coordinates are usually applied for regional and global sea circulation applications. The chart shows the computational mesh and bathymetry for the planet Earth generated by the MIKE Zero Mesh Generator

MIKE 21 & MIKE 3 Flow Model FM - Hydrodynamic Module

The Hydrodynamic Module provides the basis for computations performed in many other modules, but can also be used alone. It simulates the water level variations and flows in response to a variety of forcing functions on flood plains, in lakes, estuaries and coastal areas.

Application Areas

The Hydrodynamic Module included in MIKE 21 & MIKE 3 Flow Model FM simulates unsteady flow taking into account density variations, bathymetry and external forcings.

The choice between 2D and 3D model depends on a number of factors. For example, in shallow waters, wind and tidal current are often sufficient to keep the water column well-mixed, i.e. homogeneous in salinity and temperature. In such cases a 2D model can be used. In water bodies with stratification, either by density or by species (ecology), a 3D model should be used. This is also the case for enclosed or semi-enclosed waters where wind-driven circulation occurs.

Typical application areas are

- Assessment of hydrographic conditions for design, construction and operation of structures and plants in stratified and non-stratified waters
- Environmental impact assessment studies
- Coastal and oceanographic circulation studies
- Optimization of port and coastal protection infrastructures
- Lake and reservoir hydrodynamics
- Cooling water, recirculation and desalination
- Coastal flooding and storm surge
- Inland flooding and overland flow modelling
- Forecast and warning systems

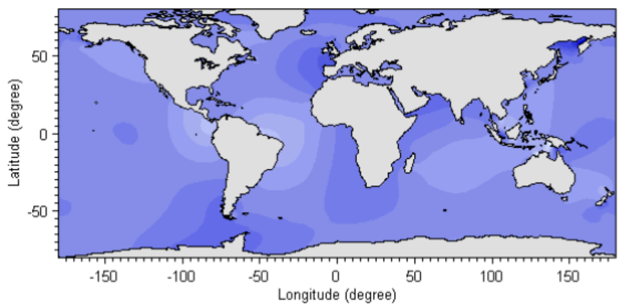

Example of a global tide application of MIKE 21 Flow Model FM. Results from such a model can be used as boundary conditions for regional scale forecast or hindcast models

APPENDIX A-4

Drift Bottle Observations in Northumberland Strait, Gulf of St. Lawrence[1]

BY L. M. LAUZIER

Fisheries Research Board of Canada
Biological Station, St. Andrews, N.B.

ABSTRACT

Drift bottles have been released at fixed stations and during cruises in Northumberland Strait from 1960 to 1963. From the 2741 releases, there have been 1213 recoveries before the winter seasons. The overall high percentage recovery (44%) and the large number of returns not far from the point of release and within a short time after releases are featured.

The drift bottle recoveries suggest a surface non-tidal drift through Northumberland Strait from the northwest and west to the southeast and east. An outward drift into the Gulf of St. Lawrence, along the northwest coast of Prince Edward Island is inferred.

The speeds of the drift were generally greater than 3 miles a day on the average. They reached 5 miles a day (0.2 knot).

RÉSUMÉ

Plusieurs lancers de bouteilles dérivantes ont été faits dans le détroit de Northumberland, de 1960 à 1963, à de nombreux points échelonnés lors des croisières ainsi que quotidiennement à des points fixes. On a retrouvé, avant l'hiver, 1213 des 2741 bouteilles lancées. La grande moyenne du pourcentage des bouteilles retrouvées était élevée, 44%. Les nombreuses découvertes à une faible distance du lancement et la courte durée des dérives sont caractéristiques.

On peut déduire des trajets des bouteilles une dérive des eaux superficielles le long du détroit de Northumberland, du nord-ouest et de l'ouest, vers le sud-est et l'est. Un mouvement de sortie des eaux de surface du détroit dans le golfe Saint-Laurent semble aussi être une déduction logique.

Les vitesses de dérives sont habituellement plus grandes que 3 milles par jour, en moyenne. Elles peuvent atteindre 5 milles par jour (0.2 noeud).

INTRODUCTION

NORTHUMBERLAND STRAIT, lying between the Prince Edward Island and New Brunswick–Nova Scotia coasts (Fig. 1), is an important commercial fisheries area for lobster and herring. Over the past 15 years a study of abundance and distribution of lobster larvae in the northern sector has been the main biological effort (Scarratt, 1964). The program included concurrent monitoring of oceanographic conditions and drift bottle experiments during 4 years, 1960–63. Earlier circulation studies in the Strait have been reported by Dawson (1913) and Farquharson (1959, 1962).

The purpose of the present study is to show seasonal and year-to-year changes of the non-tidal drift in the northern sector of Northumberland Strait and its relation to the drift in the central and eastern sectors of the Strait,

[1]Received for publication September 17, 1964.

as well as to that of the outside waters. The study was initiated to assist biologists interested in the circulation as it affects the biological content of the waters and the production of certain commercial species in the area. The results described here are pertinent to a very thin layer of surface waters. Work is being carried out to extend observations to a deeper layer and also along the bottom.

DRIFT BOTTLE RELEASES

Figure 1 shows the segmentation of Northumberland Strait referred to in this paper. The releases by segments were:

1. In northern Northumberland Strait (Northern and Egmont Bay segments).

   For 4 years, starting in 1960, regular releases of drift bottles were made repeatedly at one station from the end of May to October, and at two additional stations from June to September. The total number of releases every year at these stations in the northern segment varied from 116 to 206. This is called the *Pandalus* series. In June 1963, a large-scale release of 204 bottles was made at 32 positions covering both segments.

2. In central Northumberland Strait (Central segment).

   During 1961 and 1962, daily releases of drift bottles were made between Cape Tormentine, N.B., and Port Borden, P.E.I., from CNR

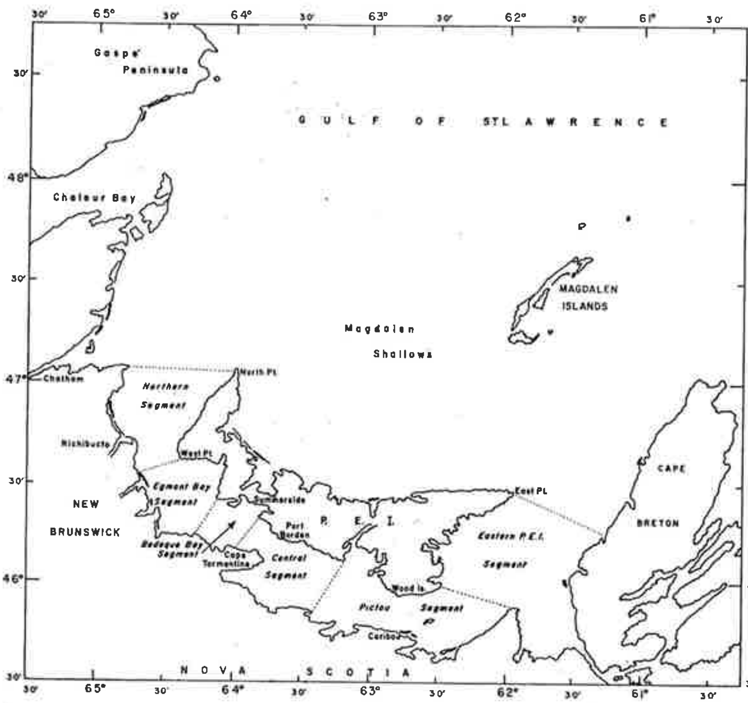

FIG. 1. Map of area showing the segmentation of Northumberland Strait used in this paper.

Abegweit (*Abegweit* series). From July to December 1961 and June to December 1962, 710 and 360 bottles were released, respectively.

3. In eastern Northumberland Strait (Pictou and Eastern P.E.I. segments).

   From May to December 1962, daily releases of drift bottles in the Pictou segment between Caribou, N.S., and Wood Islands, P.E.I., totalled 780 (*Selkirk* series). In June 1963, 46 bottles were released at 7 stations covering the Eastern P.E.I. segment.

4. Outside Northumberland Strait.

   During seven cruises, between 1959 and 1963, 974 bottles were released north of Northumberland Strait, along the New Brunswick coast, and at the entrance of Bay of Chaleur up to the Gaspé Peninsula in a strip 40–45 miles wide. A total of 99 and 90 bottles were released, respectively, in 1960 and 1963 between Prince Edward Island and the Magdalen Islands.

ANALYSIS OF RECOVERIES

Spatial Distribution and Inferred Drift

The overall percentage of the recoveries made in the same year as the releases was maximum for releases made in northern Northumberland Strait, at 54%. From releases made in central and eastern sectors of the Strait, recoveries were 46% and 27%, respectively. A certain number of recoveries was made after a winter season, approximating 3%, 7%, and 3% from the northern, central, and eastern sectors, respectively. Most of these bottles which were recovered in Northumberland Strait had been released in the last quarter of the year. Table I gives a summary of releases and recoveries from the fixed stations.

Table I. Summary of releases and recoveries of drift bottles from fixed stations in Northumberland Strait.

	Released	Recovered	
	No.	No.	%
Pandalus series			
1960 May–October	172	100	58
1961 May–November	206	108	52
1962 May–November	160	96	60
1963 April–October	116	51	44
Abegweit series			
1961 July–December	710	336	48
1962 June–December	360	154	43
Selkirk series			
1962 May–December	780	213	27

NORTHERN NORTHUMBERLAND STRAIT

The recoveries from the three fixed stations of the *Pandalus* series are illustrated in Fig. 2 and 3. These are seasonal recoveries totalled independently of the month of release. The distribution of recoveries by season of release would be very slightly different from that of Fig. 2 and 3, because of the short time between release and recovery.

More recoveries were made on the Prince Edward Island side than on the New Brunswick side of the Strait, indicating an easterly component of the drift of surface waters. Generally 50% or more of the recoveries — 61% on the average — are recorded in the area of release. Within the northern segment, the recoveries infer either a cyclonic eddy or a southerly drift along the New Brunswick coast and a northeasterly drift along the Prince Edward Island coast. This northeasterly movement of the surface waters is no doubt the main avenue for bottles drifting out of the northern Strait towards the Magdalen Islands, Newfoundland, Cape Breton, and the north coast of Prince Edward Island.

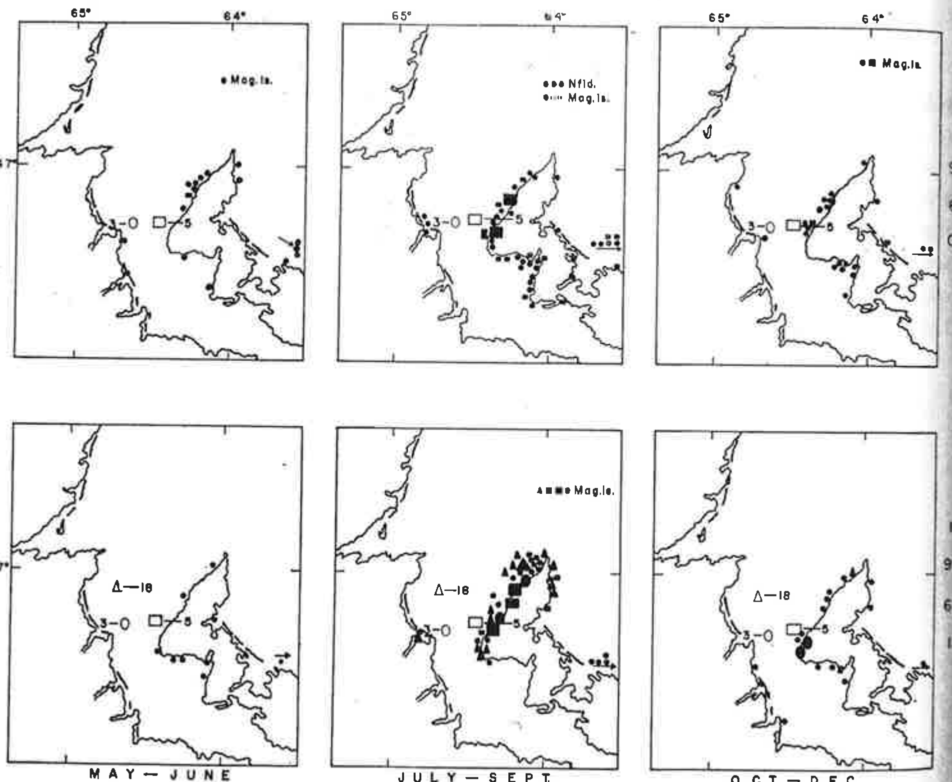

FIG. 2. Distribution of drift bottle recoveries, *Pandalus* series, from May to December 1960 and 1961. Open symbols: release stations 3, 5, and 18; closed symbols: recoveries. A small symbol represents one recovery, and a large symbol represents five recoveries.

From recoveries to the south, it is inferred that very few of the bottles that drifted into the Egmont Bay segment drifted further into the Bedeque Bay segment. The circulation in the Egmont Bay segment seems to be that of an eddy with inflow from the north along the New Brunswick coast and main outflow to the north along the Prince Edward Island coast. A predominant easterly drift is inferred from the large number of recoveries along the Prince Edward Island coast.

Even though the releases at fixed stations are few, the rates of recovery, 40–70%, are sufficient to show seasonal and year-to-year variations. The relative number of recoveries on the New Brunswick side of Northumberland Strait has a tendency to increase from summer to autumn. As shown in Table II, the percentage recovery from fixed station releases has a tendency to be minimum for July and maximum for September. The low percentage in July seems to be associated with a small proportion of recoveries within the area of releases, the northern segment, and a large proportion of recoveries away from it, either outside the Strait or in the Egmont Bay and Bedeque segments. However, a seasonal high percentage recovery is not necessarily associated

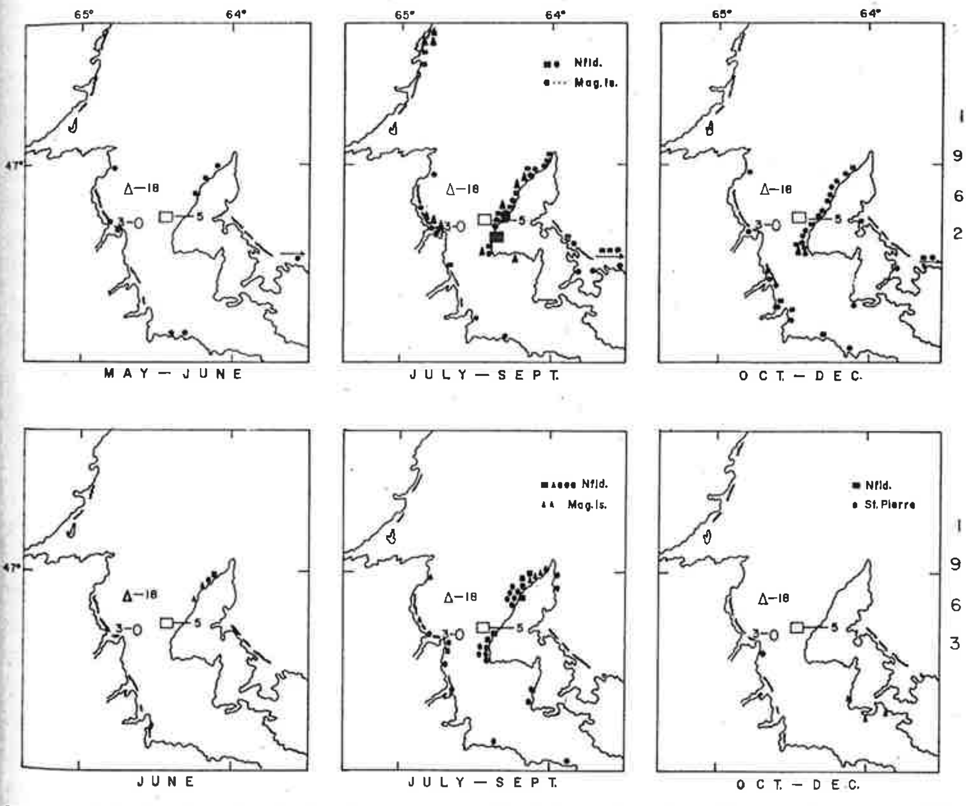

FIG. 3. Distribution of drift bottle recoveries, *Pandalus* series, from May to December 1962 and 1963. Open symbols: release stations 3, 5, and 18; closed symbols: recoveries. A small symbol represents one recovery, and a large symbol represents five recoveries.

TABLE II. Drift bottle recoveries from releases made during July and September in the northern segment, 1960–64.

	July	September
Number of releases:	128	86
Recoveries:		
in northern segment (area of release)	20	33
in Egmont Bay and Bedeque segments	13	18
outside Northumberland Strait	18	10
Total number	51	61
Percentage recoveries	40	71

with a large proportion of recoveries within the area of release. The conditions which seem to be prevalent in July are those of either divergence or dispersion from the area or rapid flushing of the area.

As shown in Fig. 2 and 3, during 1961 and 1963, a relatively high proportion of recoveries occurred in the northern segment, the area of release, associated with a relatively low proportion in the Egmont Bay segment and outside the Strait. Opposite conditions were predominant in 1960 and 1962. In 1963 the overall percentage recovery was the smallest in 4 years, and the July conditions described earlier still existed. Other contrasting conditions are also shown in the Magdalen Islands and Newfoundland recoveries; they amount to 16% of all the outside recoveries in 1962 and 80% in 1963. This could be an indication of stronger circulation over the Magdalen Shallows in 1963 than in 1962.

The recoveries from the releases made during June 1963 at several stations covering both northern and Egmont Bay segments are grouped in Table III. They infer a circulation pattern similar to that deduced from the fixed stations releases and recoveries; namely, a strong movement from west to east in the northern and Egmont Bay segments, and as an eddy in the northern segment confirming a northeasterly current along the Prince Edward Island coast. However, the inferred drift of surface waters towards the central segment of the Strait, and even east of it, is more definite than previously observed. For the bottles released in the northern segment, 31% of all the recoveries were made south of the Egmont Bay segment, as compared with the previous average of 2%. For the bottles released in the Egmont Bay segment, 86% followed a southeasterly direction towards the central and eastern sectors of the Strait. As a corollary, the inferred drift of surface waters to the east past North Point, P.E.I., was rather restricted, since only 10% of all the recoveries were recorded outside the Strait. The conditions in the second half of June 1963 were those

TABLE III. Drift bottle recoveries from releases made in June 1963 in northern and Egmont Bay segments.

	Northern segment	Egmont Bay segment
Number of releases	156	48
Number of recoveries in:		
Northern segment		
P.E.I. side	37	–
Mainland	–	–
Egmont Bay segment		
P.E.I. side	20	3
Mainland	3	1
Bedeque Bay segment		
P.E.I. side	3	–
Mainland	12	5
Central segment		
P.E.I. side	5	7
Mainland	8	5
Pictou and eastern P.E.I. segments		
P.E.I. side	4	2
Mainland	1	5
Outside	12	1

of relatively strong circulation through Northumberland Strait. This had not been observed before. It is not surprising that such differences should occur between recoveries from cruise-type releases involving a large number within a short time, and recoveries from fixed station-type releases involving repeated releases of a small number of bottles at regular intervals. The former gives inferences of the circulation over a short period of time, the latter of the average circulation over a wide range of conditions.

CENTRAL NORTHUMBERLAND STRAIT

A large number of drift bottles was released in the central part of Northumberland Strait between Cape Tormentine, N.B., and Port Borden, P.E.I. This was termed the *Abegweit* series. For the summer releases, 1961 and 1962, the percentage recovery (67%) was greater, on the average, than for the *Pandalus* series (52%). The percentage recovery decreased for those released during the autumn.

The seasonal recoveries in 1961 and 1962 are shown in Fig. 4 and 5, respectively. The salient features of the recoveries are: (1) their large proportions on the Prince Edward Island side in comparison with the New Brunswick side; (2) their concentrations at a short distance from the point of release; (3) their relative spread to the east and their absence in the Egmont Bay segment. The inferred predominant drift from the mainland to Prince Edward Island was relatively stronger in 1961 than in 1962. This west–east drift seems to weaken during the autumn (October–December) as compared with the summer (July–September). The same variations were inferred from recoveries of the *Pandalus* series.

The *Abegweit* series, similar to the *Pandalus* series, inferred a somewhat restricted drift. However, there is an inference of a definite southeasterly drift from the central segment into the Pictou segment but only occasionally further to the east. The much less frequent westerly drift towards the Bedeque Bay segment seems to increase from summer to autumn.

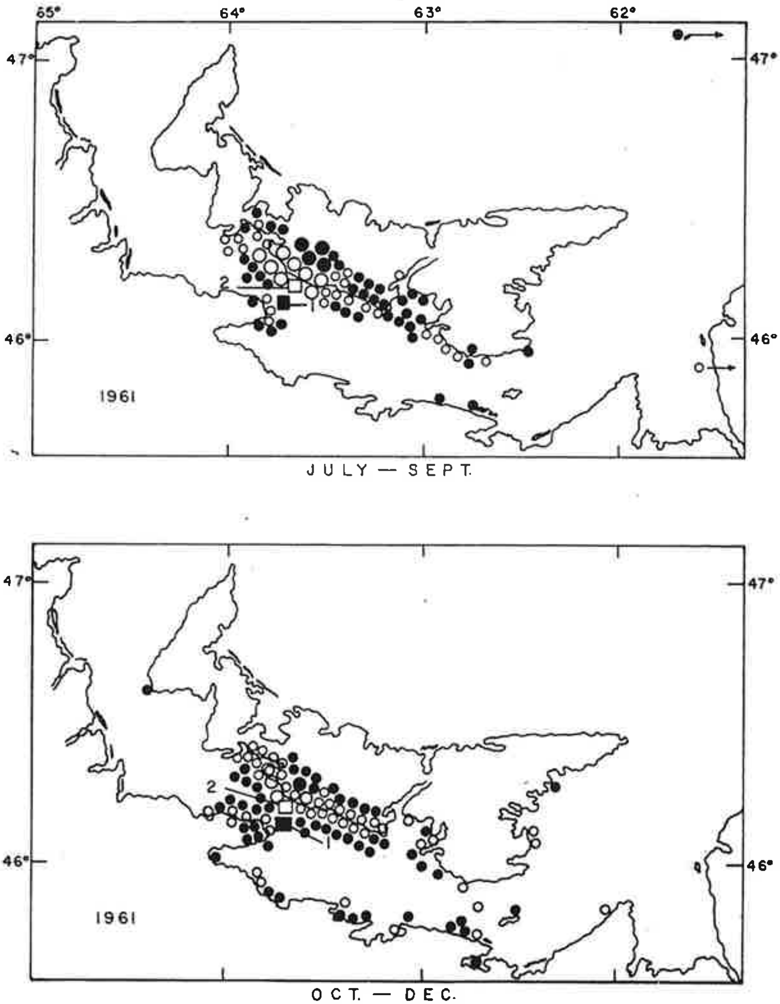

FIG. 4. Distribution of drift bottle recoveries, *Abegweit* series, from July to December 1961. Squares: release stations 1 and 2; circles: recoveries. A small circle represents one recovery, and a large circle represents ten recoveries.

EASTERN NORTHUMBERLAND STRAIT

In 1962 only, the eastern sector of Northumberland Strait was studied at the same time as the central and northern sectors. The overall percentage recovery from the *Selkirk* series released between Wood Islands, P.E.I., and Caribou, N.S., was 27%, the lowest of the three series in Northumberland Strait. It was 35% for summer month releases, still the lowest of the three series.

As inferred from the recoveries (Fig. 6), a predominant drift from the mainland to Prince Edward Island is one of the features of spring and summer seasons. There is almost a reverse of this drift during autumn. There is also

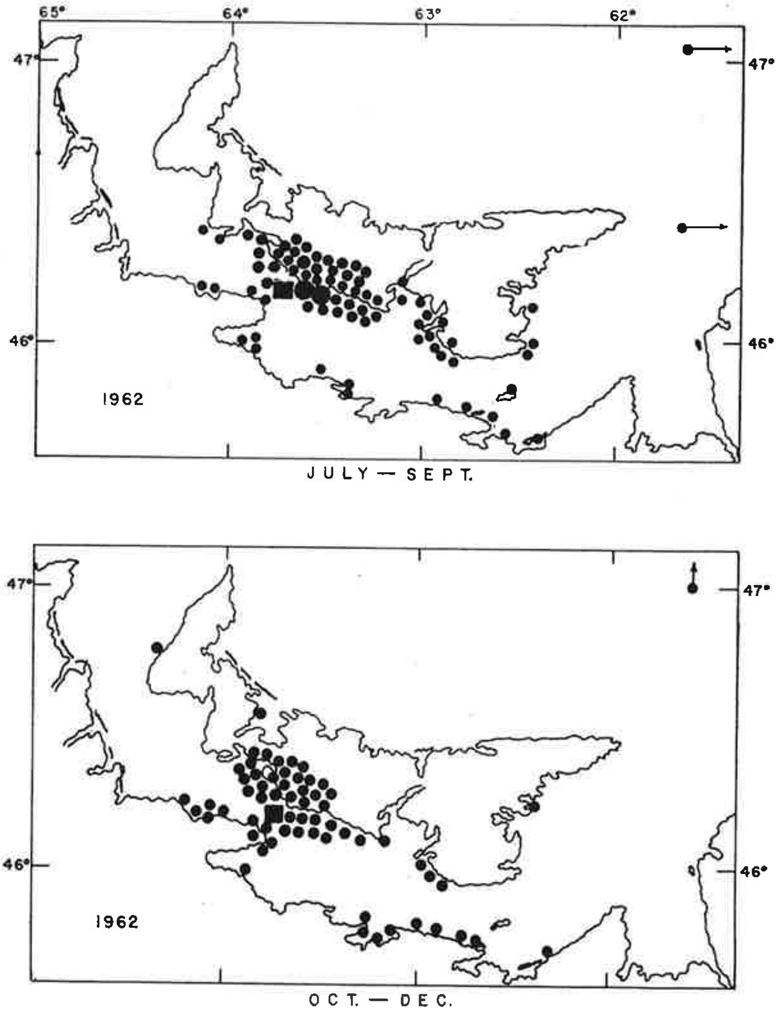

FIG. 5. Distribution of drift bottle recoveries, *Abegweit* series, from July to December 1962. Squares: release station; circles: recoveries. A small circle represents one recovery, and a large circle represents ten recoveries.

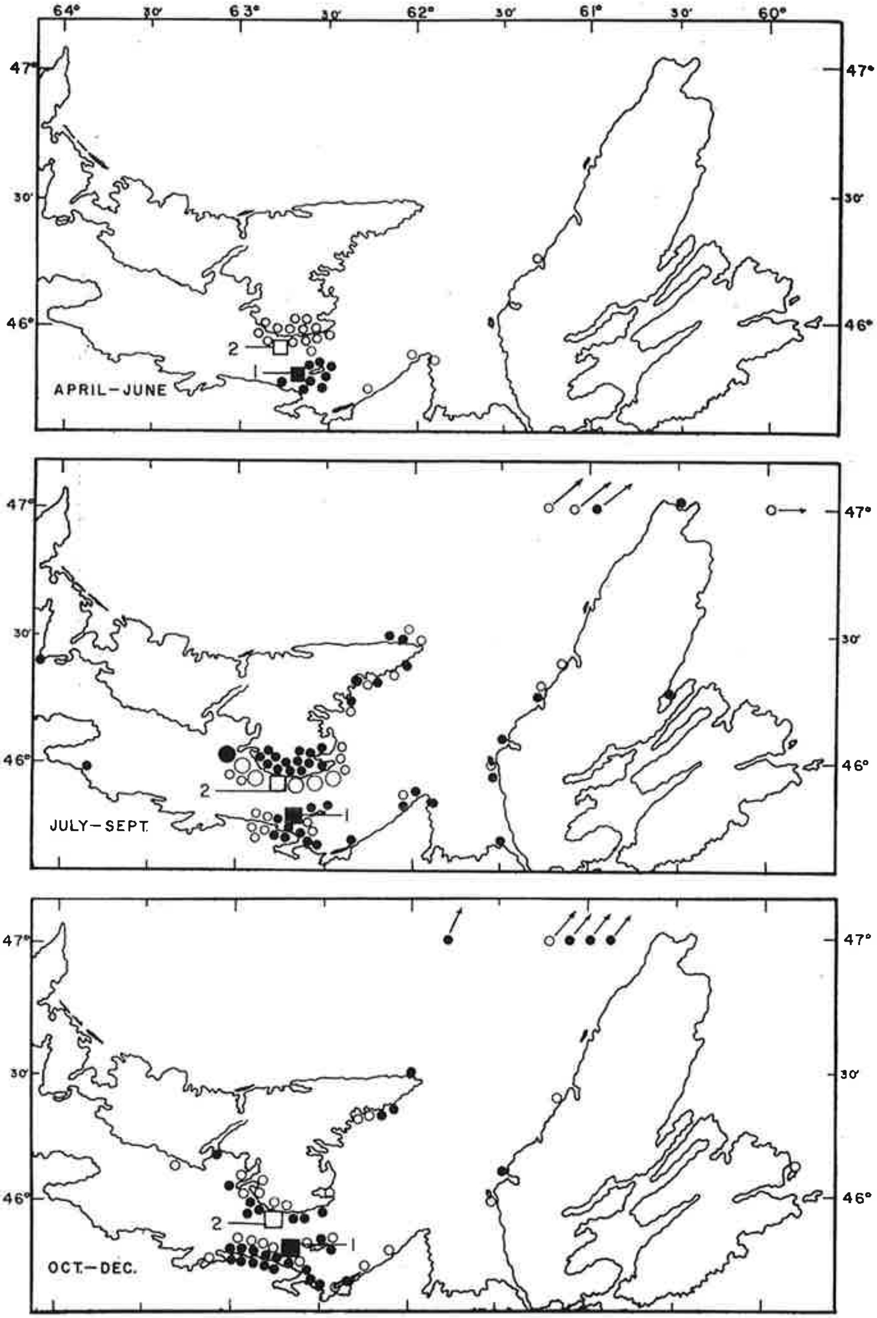

FIG. 6. Distribution of drift bottle recoveries, *Selkirk* series, from April to December 1962. Squares: release stations 1 and 2; circles: recoveries. A small circle represents one recovery, and a large circle represents ten recoveries.

a certain amount of westward drift but it hardly extends into the central segment. A definite easterly drift from the Pictou segment to the eastern P.E.I. segment and beyond is inferred. From the summer releases, 22% of all the recoveries are recorded to the east more than 20 miles from the point of release, and 15% more than 40 miles away. At the same time 75% of all recoveries were observed within 15 miles of the point of release. There is no strong evidence of drift on the south side of the Strait opposite to that on the north side.

In June 1963, 46 drift bottles were released at seven stations in the eastern P.E.I. segment at approximately the same time other releases were conducted in the northern end of the Strait. A percentage recovery of 50% was recorded for the releases in the eastern P.E.I. segment. More than half of these recoveries infer an easterly drift towards outside the area of release, while the others infer a westerly drift, up to 25 miles west of the point of release. There are similarities between the northern segment and the eastern P.E.I. segment. To someone in Northumberland Strait, looking towards the open Gulf, there seems to be a southward drift on the left hand side of the segments and a northeasterly drift on the right hand side. The presence of cyclonic eddies is inferred in both cases.

OUTSIDE RELEASES

On several occasions, drift bottles were released during cruises in the vicinity of Northumberland Strait. The surface non-tidal drift over the southwestern Gulf of St. Lawrence as inferred from drift bottle recoveries seems to be generally to the south and to the east (Bumpus and Lauzier, 1964). It is important to assess the contribution of outside waters to Northumberland Strait. From 974 bottles released north of the Strait, 247 bottles were recovered (before winter) in various parts of the Gulf. Less than 9% (21) of all recoveries or 2.2% of all releases were reported from Northumberland Strait, most of them in the northern segment, and none as far as the central segment. These originated only from some of the cruises.

The inferred circulation in the area north of Northumberland Strait seems to be in most cases to the southeast or east and in at least 10% of the cases to the south towards the Strait. However, it is impossible to estimate the extent of a southerly drift which makes a "u-turn" in northern Northumberland Strait: into the northern segment along the New Brunswick coast and out into the Gulf again along the Prince Edward Island coast. It seems that Northumberland Strait does receive on the average a rather small "share" of the surface waters just north of it.

Time Distribution and Inferred Speed

The overall percentage recoveries for the summer month releases in 1962 were 63%, 61%, and 35% for the *Pandalus*, *Abegweit*, and *Selkirk* series, respectively. The time taken to recover a definite proportion of released bottles varies from one series to the other, depending on their location in the Strait. From the *Abegweit* series, 25% of the releases in the central segment were recovered within 10 days; from the *Pandalus* series, 25% of the releases in the northern segment were recovered in 17 days; and from the releases in Pictou segment, the *Selkirk* series, 25% were recovered in 23 days.

Such a short lifetime afloat of an *Abegweit* bottle is not surprising if one considers the geographical location of the points of release, the predominant drift from the mainland to Prince Edward Island, and the rate of recovery within 10 miles of the point of release — 67% of all recoveries. It took a longer time to recover 25% of the bottles from *Pandalus* and *Selkirk* series because these were released in wider parts of the Strait which are adjacent to the open Gulf. The time given for "25% recovery" is not constant for a given segment but the shorter period always seems to be characteristic of the *Abegweit* series, released in the central segment.

The inferred speed of surface drift has been calculated in two different ways, after eliminating the recoveries recorded within 10 miles from the point of release. First, an average speed was computed from the fastest bottles (the upper third of the speed frequency) irrespective of the distance travelled outside the 10-mile radius; this was the technique used by Bumpus and Lauzier (1964). Second, another average speed was computed from most of the bottles which had travelled a certain distance, always greater than 10 miles; some very slow ones were excluded.

In using the fastest bottles an attempt was made to show seasonal variations of speed and direction; however, no such attempt was made with the other technique. The average speeds are listed in Table IV. As expected, the speeds computed for trips longer than 20 miles are approaching the values calculated for the fastest bottles. In general, the longer the "trip", the faster

TABLE IV. Average surface drift in miles per day from June to October.

Series segment	*Pandalus* northern	*Abegweit* central	*Selkirk* Pictou
Fastest bottles[a]	4.5 (NE)	3.5	3.5
	3 (SE)		
Most bottles			
10–15-mile trips	1.6	1.3	1.8
15–20-mile trips	2.9	1.3	1.5
20–50-mile trips	3.7	3.3	2.3
>50-mile trips	3.5	–	2.7

[a]Upper third of the speed frequency and drifts of 10 miles or more.

is the drift. Possibly a short trip may be a series of drifts back and forth or drifts around an eddy and ending not too far from the point of release. A longer trip may be a more straightforward drift free from aleatory motion. It should be realized that the speed values listed here are minima and in some cases may be much smaller than the actual speed of the drift. However, they represent the speed of a thin surface layer 18–20 cm deep. The residual currents recorded by the Canadian Hydrographic Service (Farquharson, 1959) are of somewhat lower strength. They vary generally between 1 and 2 miles a day and represent the speed of a residual current at a depth of 7 m.

In the northern segment, the northeast drift always seemed to be faster than the southwest drift by a factor that varies between 1.3 and 2.5. The maximum speeds occurred in July for the northern segment and from June to August for the Pictou segment. They may reach 5 miles a day. There were no seasonal tendencies in the inferred speeds for the central segment.

DISCUSSION

Because of the high proportion of local recoveries, the three series *Pandalus*, *Abegweit*, and *Selkirk* seem to indicate that they are three "stocks" that do not "intermingle". Most recoveries infer a drift to a certain point along the Strait but very seldom further. There seems to be a drift from northwest to southeast at various points along the Strait. Bottles released in a relatively small body of water have a short average lifetime and are subjected to a high rate of recovery. From the rate of recovery, the average speed, and the distance to be travelled to go from one area of release to the other, it is possible to estimate the chances for bottles released in the central segment of the Strait to drift into another area of release. With an average speed of 2 miles a day, it would take 25 days to reach another area of release; by that time, 40–45% of the bottles released would have already been recovered. In the case of the bottles released in the northern segment, the assumed speed is higher and the rate of recovery within the first month, lower. Then 25% of the bottles released would have been recovered before being able to reach the area of release in the central segment, if all the bottles had drifted into the segments to the southeast. In fact only 15% did so. Consequently the experiment cannot demonstrate continuity of flow.

The recovery charts (Fig. 2–6) do not imply a continuous drift from one end of the Strait to the other. However, the similarities in the speeds within various segments, the consistency and some predominance of southeasterly and easterly drift, as well as the lack of long drifts westward in the central and Pictou segments infer a resultant drift of surface water in Northumberland Strait from the northwest to the southeast. Figure 7 shows the average surface circulation in Northumberland Strait as inferred from drift bottle releases and recoveries. The inference of a resultant drift from the northwest to the southeast is strengthened by consideration of the seasonal variations of salinity conditions. During the summer, a large body of relatively low salinity

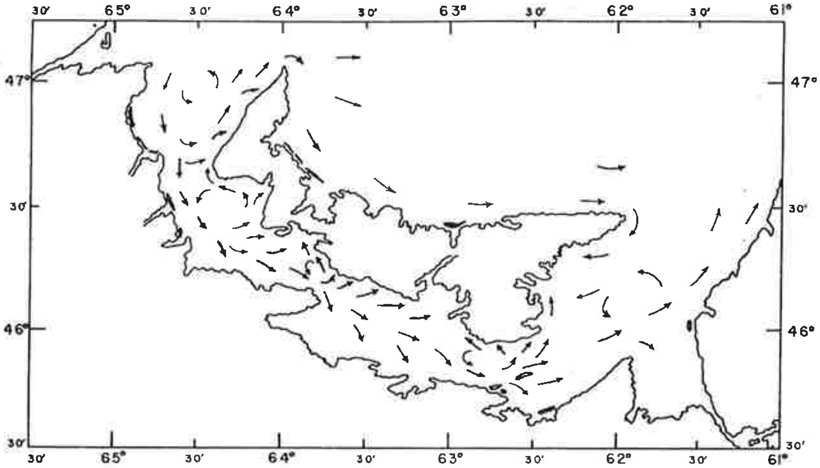

FIG. 7. The inferred non-tidal drift in Northumberland Strait.

water drifts southward over the Magdalen Shallows. A summer minimum of salinity is also observed in Northumberland Strait (Lauzier, 1957).

It was mentioned previously that, in general, the relative distribution of recoveries from the July *Pandalus* series is different from average conditions. It was presumed then that either dispersion or rapid flushing occurred in the area. Approximately at the time there is a summer minimum of salinity and a definite gradient of salinity between the western and eastern ends of Northumberland Strait which might be partly responsible for a stronger circulation through the Strait, or at least in both the northern and Egmont Bay segments.

The predominant drift in Northumberland Strait from the mainland to Prince Edward Island during the summer months was observed to diminish during the autumn all over the Strait and almost to the point of a reversal in the Pictou segment. This might be associated with the weakening of the southwest winds and the strengthening of the easterly winds in the autumn. Although the outside contributions to Northumberland Strait from the north are generally small, they were greater in June and August 1959 and May 1960 than at any other time of observation. From one cruise as many as 23% of the recoveries were reported in Northumberland Strait. In most cases, when bottles were recovered in the Strait, the resultant winds (as observed at Summerside, P.E.I.) had either a stronger easterly or a weaker southerly component than usual. When bottles released outside were not recovered in the Strait, the resultant winds seemed to have a stronger component than usual from either the south or the west. These are the only relationships found so far, between the direction of the surface drift and the resultant winds on a monthly basis.

It is assumed that the bottles drift with the water and its biological content such as lobster and herring larvae. Drift bottle observations give some of the history of particles of water (Lagrangian observations) in contrast with current-meter observations which give the history of what goes on at one point (Eulerian observations) without knowledge of origin or past history of the particles in motion. Most biological and oceanographic observations are of the Eulerian type. The circulation of the surface waters in Northumberland Strait illustrated in Fig. 7 should be taken as the most probable circulation pattern under various conditions. From the data on hand it is impossible to say how constant and how fast is the renewal of waters and the biological content in a given segment, or how long the water stays in a segment. However, eddies seem to exist at both ends of the Strait. There is a northwest–southeast drift through the Strait but it is not known if this inferred drift is counterbalanced by a reverse drift which is impossible to observe because of the prevalent onshore drift along Prince Edward Island. It is hoped that the answers to this and many other unknowns concerning water circulation in Northumberland Strait will be revealed through further research.

SUMMARY

The surface circulation in Northumberland Strait has been studied from drift bottle experiments at fixed stations and during cruises. Emphasis was given to the northern sector of the Strait, starting in 1960, but the studies covered the whole Strait in 1962. From releases of 2741 bottles in 1960 to 1963 the overall percentage recovery was 44%. The percentage recovery for a year or for the summer months was generally higher (above 60%) in the northern part of the Strait, and lower (less than 40%) in the eastern end of the Strait.

The main features of the inferred surface non-tidal drift are:

1. A general movement of the surface waters through the Strait from the northwest and west to the southeast and east.
2. A predominant drift from the mainland to Prince Edward Island, stronger in the summer than in the autumn.
3. A cyclonic eddy in the northern entrance of the Strait with a southerly drift along the New Brunswick coast and northeasterly drift along the Prince Edward Island coast, the latter being the main avenue towards the open Gulf.
4. Other eddies are suggested mainly south of West Point, P.E.I., and at the eastern entrance of the Strait.
5. The speeds seem to vary seasonally in certain parts of the Strait. They are generally greater than 3 miles a day on the average, and may reach 5 miles a day.

In general the rate of drift bottle recoveries is high for the releases made in the central part of the Strait, where 25% of the bottles released are recovered within 10 days. It takes 17 and 23 days to recover the same proportion of those released in the northern and southern ends, respectively.

ACKNOWLEDGMENTS

The author is indebted to Dr D.G. Wilder of the lobster investigations at the Biological Station, St. Andrews, N.B., for his assistance in organizing the drift bottle releases from M.V. *Pandalus II* starting in 1960; to the masters of *Pandalus II* (Fisheries Research Board), of *Abegweit* (Canadian National Railways), and of *Lord Selkirk* (Northumberland Ferries) for their co-operation in the task of drift bottle releases. The assistance of Messrs J.G. Clark and A.W. Brown in the organization and co-ordination of releases and in the compilation of drift bottle data is gratefully acknowledged. Drift bottle data related to outside releases in 1959 were supplied to the author by Dr Y.M.L. Jean.

REFERENCES

Bumpus, D. F., and L. M. Lauzier. 1964. Surface circulation on the continental shelf off eastern North America between Newfoundland and Florida. Folio 7. Serial Atlas of the Marine Environment, American Geographical Society, New York.

Dawson, W. B. 1913. The currents in the Gulf of St. Lawrence. Dept. of the Naval Service, Ottawa.

Farquharson, W. I. 1959. Causeway Investigation Northumberland Strait. Report on Tidal Survey 1958. Dept. Mines and Technical Surveys, Ottawa, 137 pp.
1962. Tides, tidal streams and currents in the Gulf of St. Lawrence. Dept. Mines and Technical Surveys, Ottawa, 76 pp.

Lauzier, L. M. 1957. Variations of temperature and salinity in shallow waters of the southwestern Gulf of St. Lawrence. *Bull. Fish. Res. Bd. Canada*, No. 111, pp. 251–268.

Scarratt, D. J. 1964. Abundance and distribution of lobster larvae (*Homarus americanus*) in Northumberland Strait. *J. Fish. Res. Bd. Canada*, **21**(4): 661–680.